Séminaire de Calcul Scientifique du CERMICS

École des Ponts
ParisTech

Going beyond failure in mechanics
From bifurcation theory to strain localization and earthquake control

Ioannis Stefanou (Navier, ENPC)

19 avril 2018

Going beyond failure in mechanics

From bifurcation theory to strain localization and earthquake control

Dr Ioannis Stefanou

Laboratoire Navier, Ecole des Ponts ParisTech, IFSTTAR, CNRS UMR8205

ioannis.stefanou@enpc.fr

Earthquakes, should we care?

The Nepal 2015 EQ, M_w 7.8 :
(previous 1833)

Casualties: 9.000 killed, 22.000 injured

Damage cost: ~35% Nepal's GDP (~$10B)

Repair estimates for UNESCO monuments:
$160 million

Total direct international aid: ~$1340 million
(EU countries direct aid: ~$250 million)

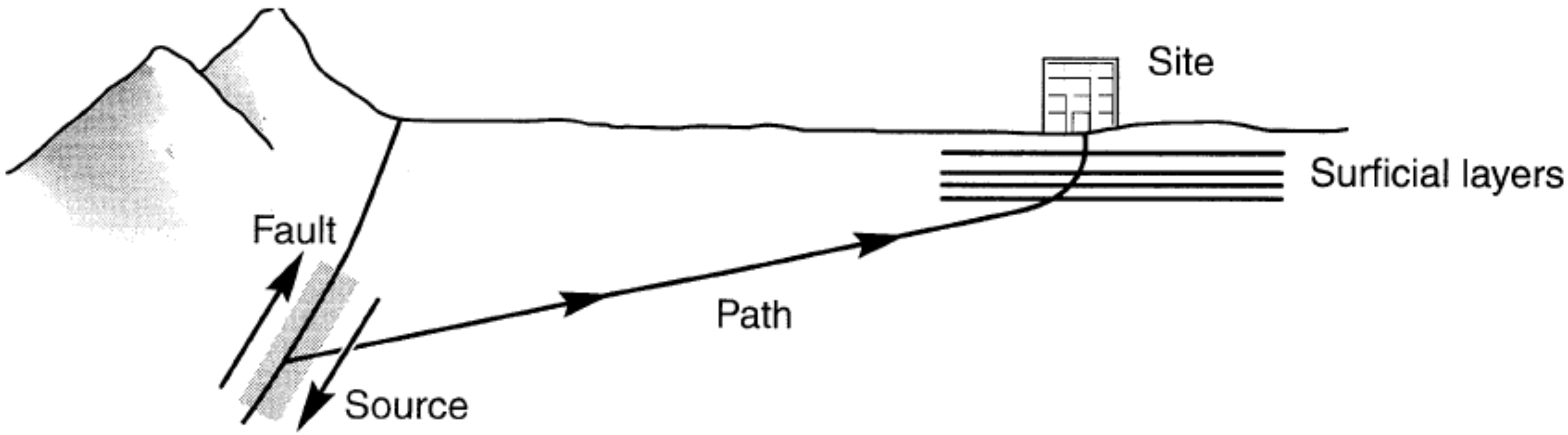

Accumulated elastic energy -> Friction (>90%) + Fault propagation + **Radiation**

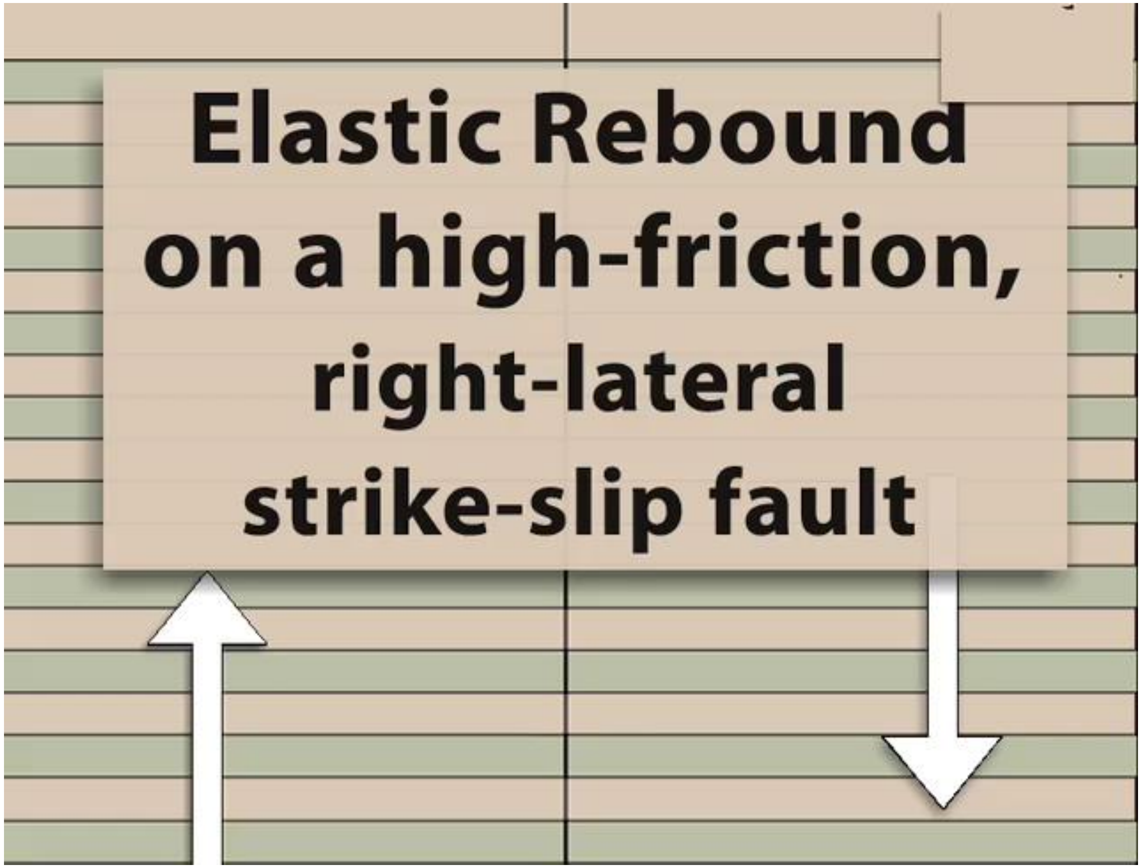

(IRIS, Incorporated Research Institution for Seismology)

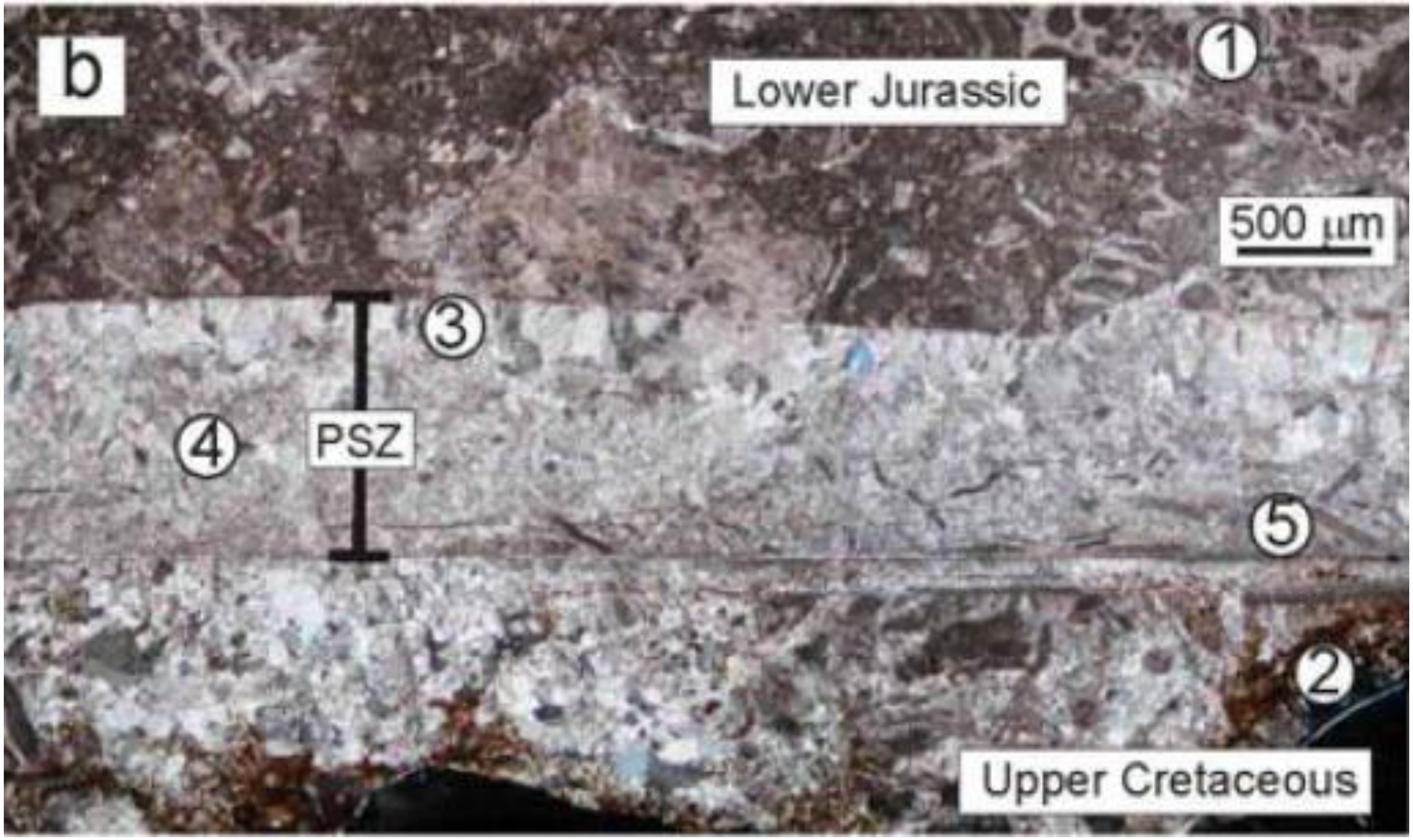

from Collettini et al., 2012, Geology

Principal slip zone (0.3 to 1mm) of Spoleto thrust fault in Central Italy 5-10km of accumulated displacement

Faults

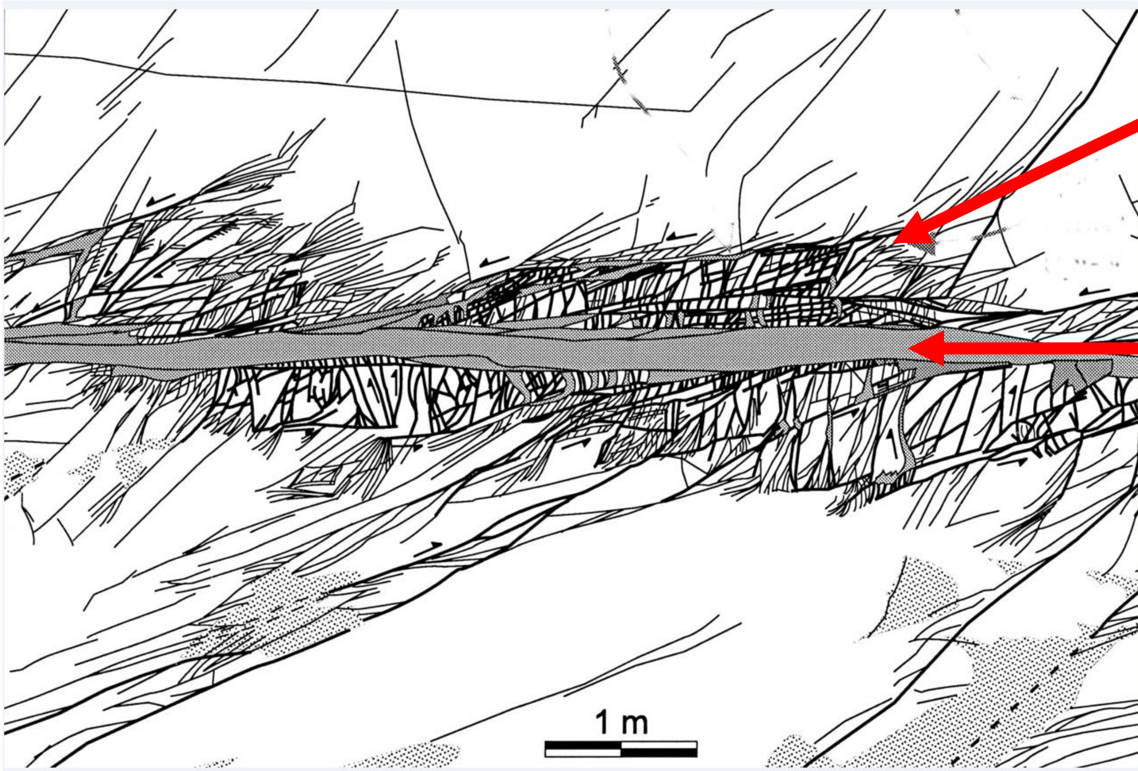

Myers et al. (1994)

Damaged zone

thickness: from ~10 m to ~1 km

Gouge

composed of very fine crushed particles, where the slip is localized thickness:
from ~1 µm to ~10 mm

"Science may be described as the art of systematic over-simplification"

Karl R. Popper

EQ nucleation - dynamic instability

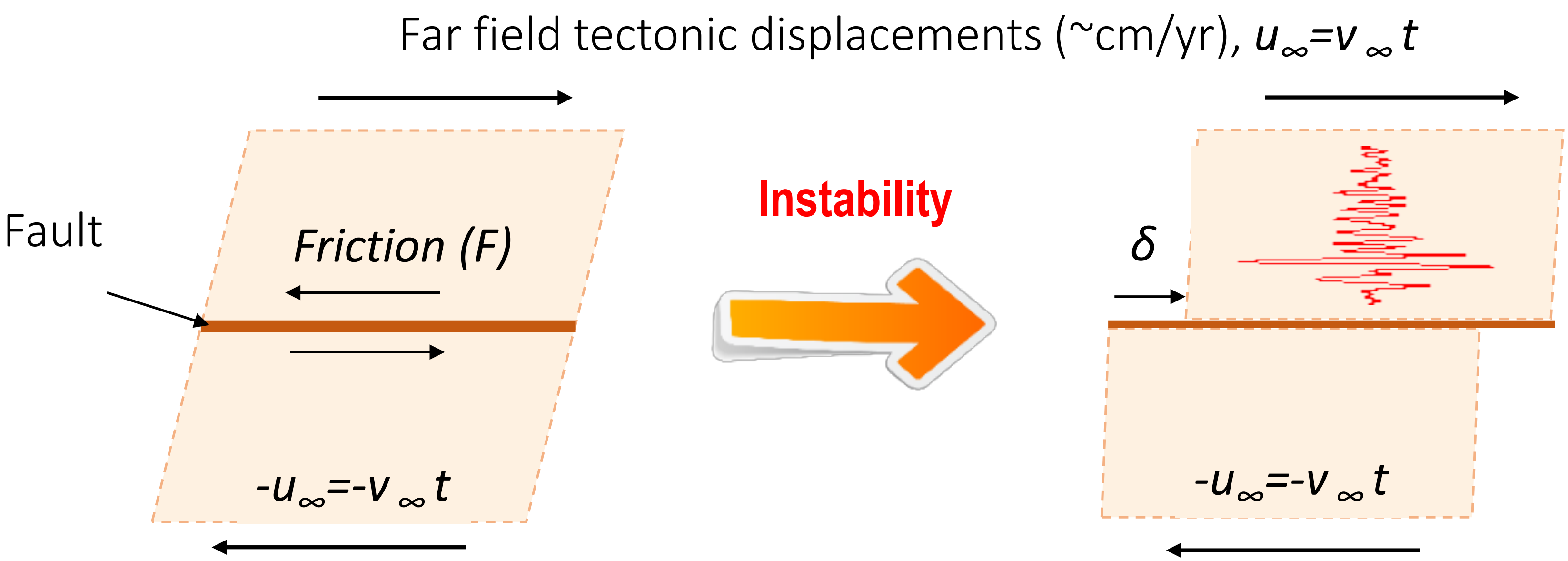

Storage of elastic energy in the crust $U_{el} \uparrow$

Sudden release of elastic energy → earthquake

The spring-slider toy model for building understanding

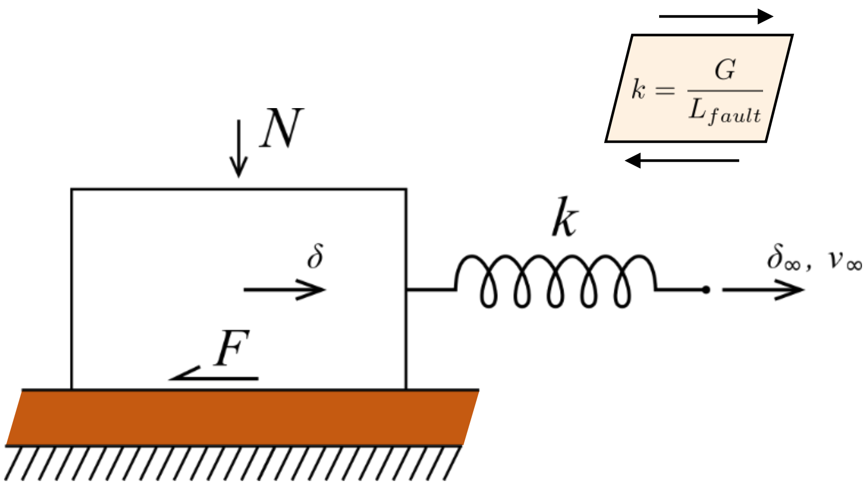

Reid, 1910

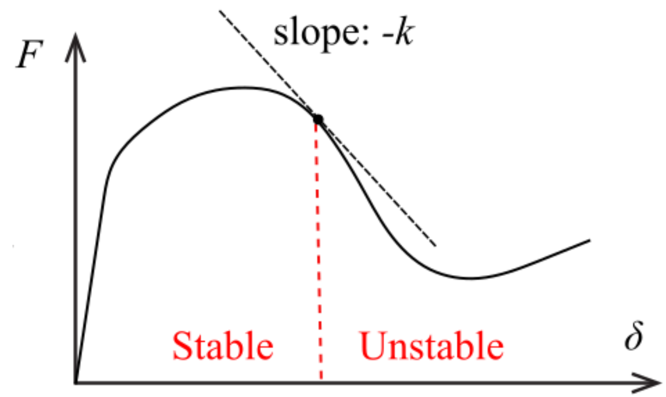

From bifurcation theory we retrieve the classical condition for instability of steady state slip motion:

$$\frac{\partial F(\delta)}{\partial \delta} < -k$$

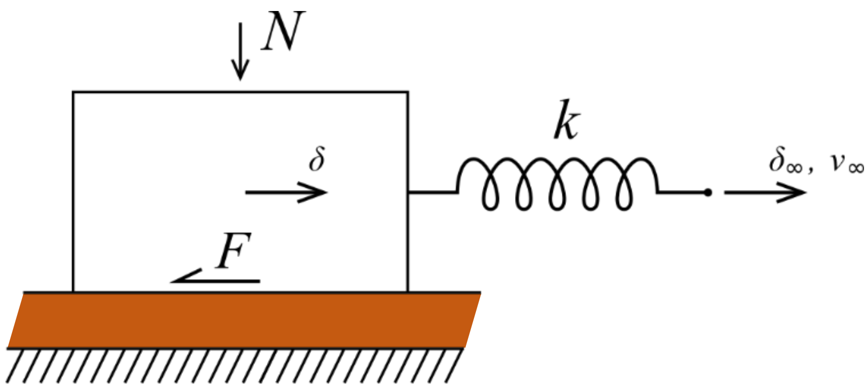

But of course, friction depends on many factors:

$$F(\boldsymbol{\delta}, \dot{\boldsymbol{\delta}}, \textbf{pore pressure}, \textbf{temperature}, \textbf{grain size}, \mathit{healing}\ \ldots)$$

For instance when $\dfrac{\partial F(\dot{\delta})}{\partial \dot{\delta}} < 0$ (velocity weakening) steady state slip is

(unconditionally) unstable

Weakening mechanisms and earthquake nucleation

For the nucleation of unstable, seismic slip we need somehow a sufficient weakening of the shear resistance of the fault zone.

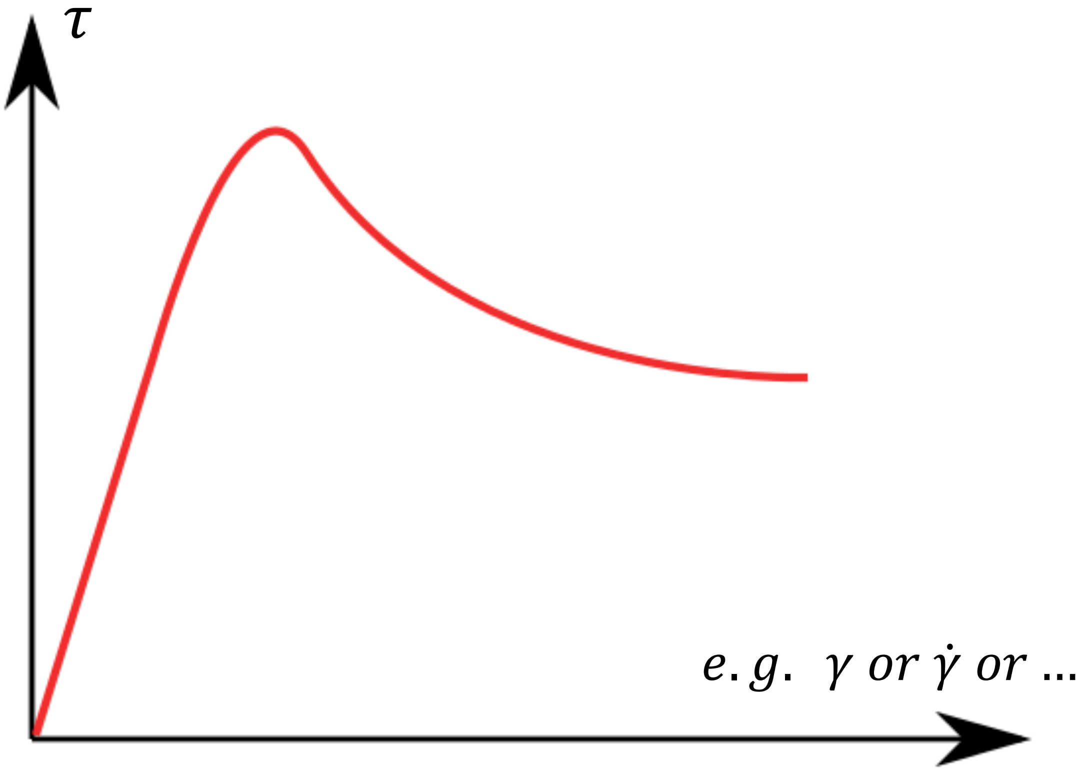

Examples of weakening and multiphysical couplings

- **Mechanical softening** (e.g. reduction of the friction angle, velocity weakening, RSF, *Dieterich, 1978, Rice, J. R., & Ruina, A., 1983, Marone et al., 1990, Scholz, 1998*)

- **Thermal pressurization** of pore fluids (*Lachenbruch, 1980, Vardoulakis, 2002, Sulem et al. 2005, Rice 2006, Platt et al. 2014a,b*)

- **Thermal decomposition of minerals**: dehydration of clay minerals (*Brantut et al., 2008*), decomposition of carbonates (*Sulem & Famin, 2009, Collettini et al., 2014, Veveakis et al. 2014, Platt et al. 2015*).

- **Flash heating** and shear weakening at micro-asperity contacts (*Rice, 1999, 2006, Spagnuolo et al., 2016*).

- **Lubrication** due to the formation of a ‘gel-like’ layer in wet silica rich fault zones (*Di Toro et al., 2004*).

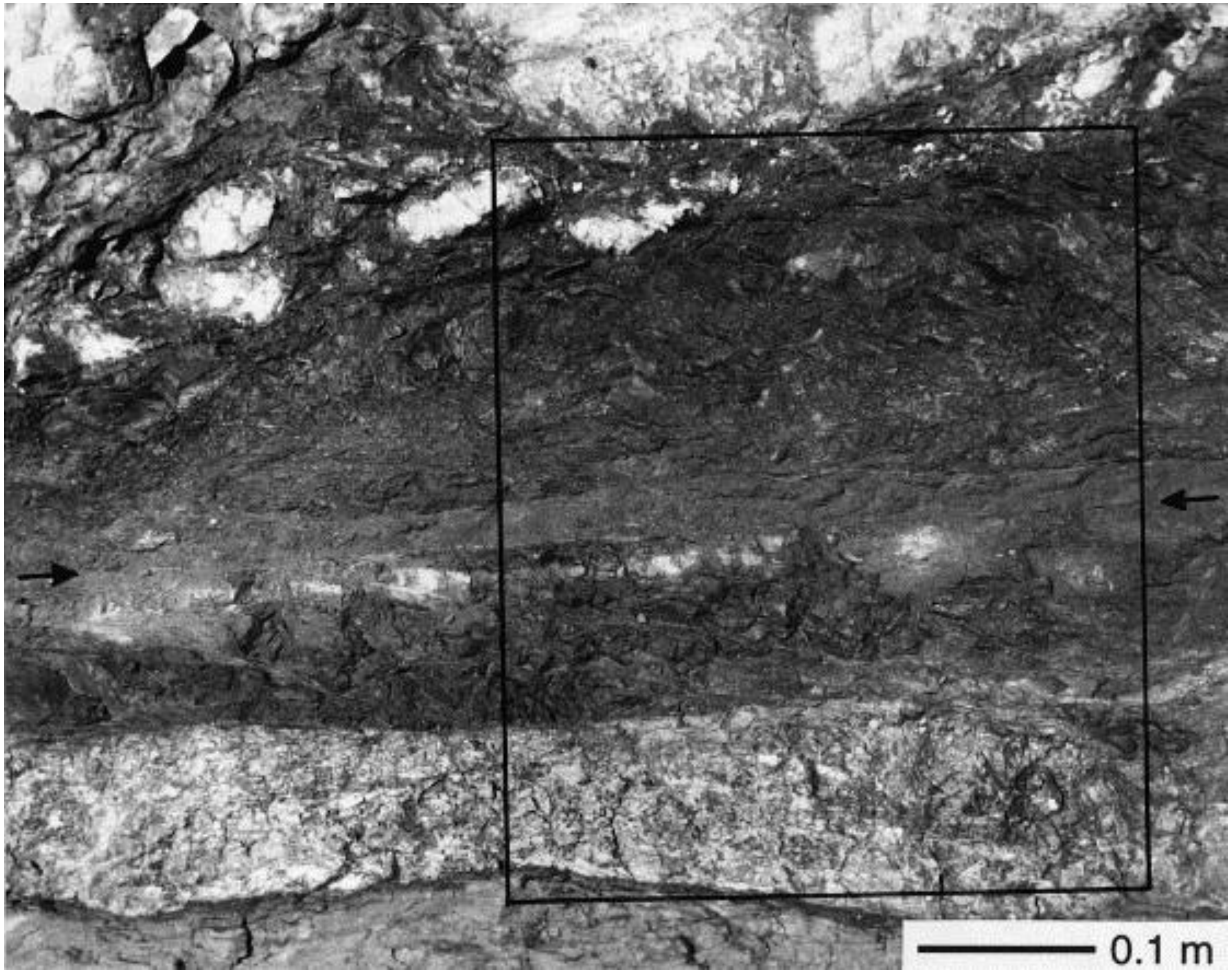

All these couplings and phenomena take place in a zone of finite thickness

from Chester & Chester. (1998), Tectonophysics

Thickness of Principal Slip Zones in active faults

- Observed in many faults, but the sizes depend strongly on physical properties of the gouge.

Fault system	Thickness of the PSZ	Reference
Median Tectonic Line, Japan	3 mm	Wibberley et al., 2003
Chelungpu fault, China	50-300 µm	Heermance et al., 2003
Longmenshan fault, China	1cm	Li et al. , 2013
Punchbowl fault, USA	100-300 µm	Chester et al., 2003
Northern Apennines, Italy	10-40 µm	De Paola et al., 2008

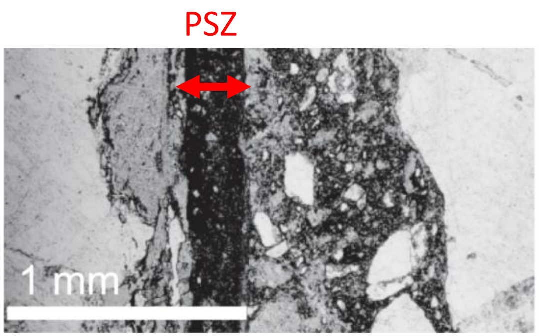

PSZ in Nevada (Shipton et al., 2006)

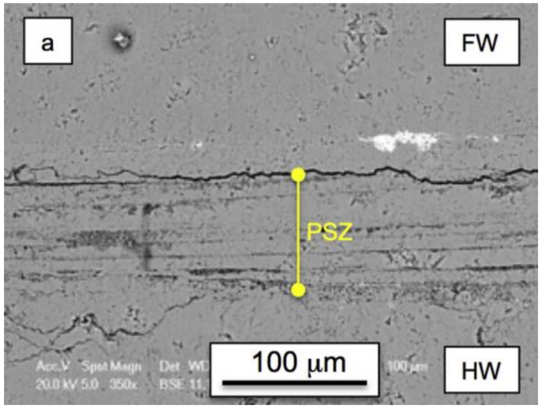

PSZ in M. Maggio, Italy (Collettini et al., 2014)

Importance of the size of the microstructure

Field and experimental observations show that the shear band thickness is associated with **grain size**

Grain size affects the different physical phenomena: chemistry kinetics, specific surface evolution, pore pressure, porosity, etc...

⇨ We need a theory that takes into account the microstructure and its evolution

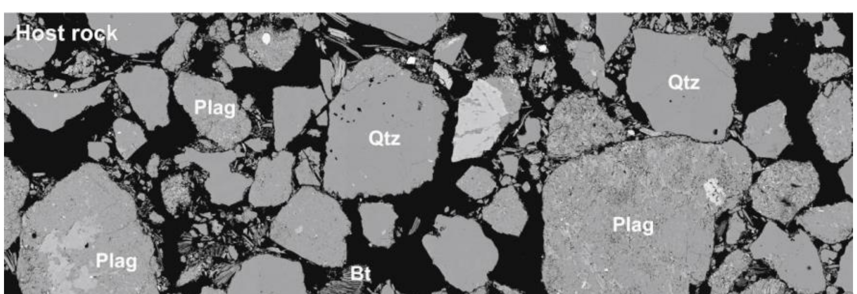

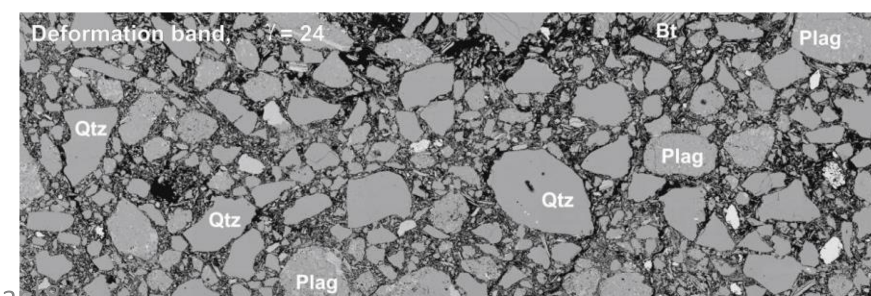

Exner and Tschegg (2012)

Theory of micromorphic continua

&

Cosserat continuum

Micromorphic (generalized) continua

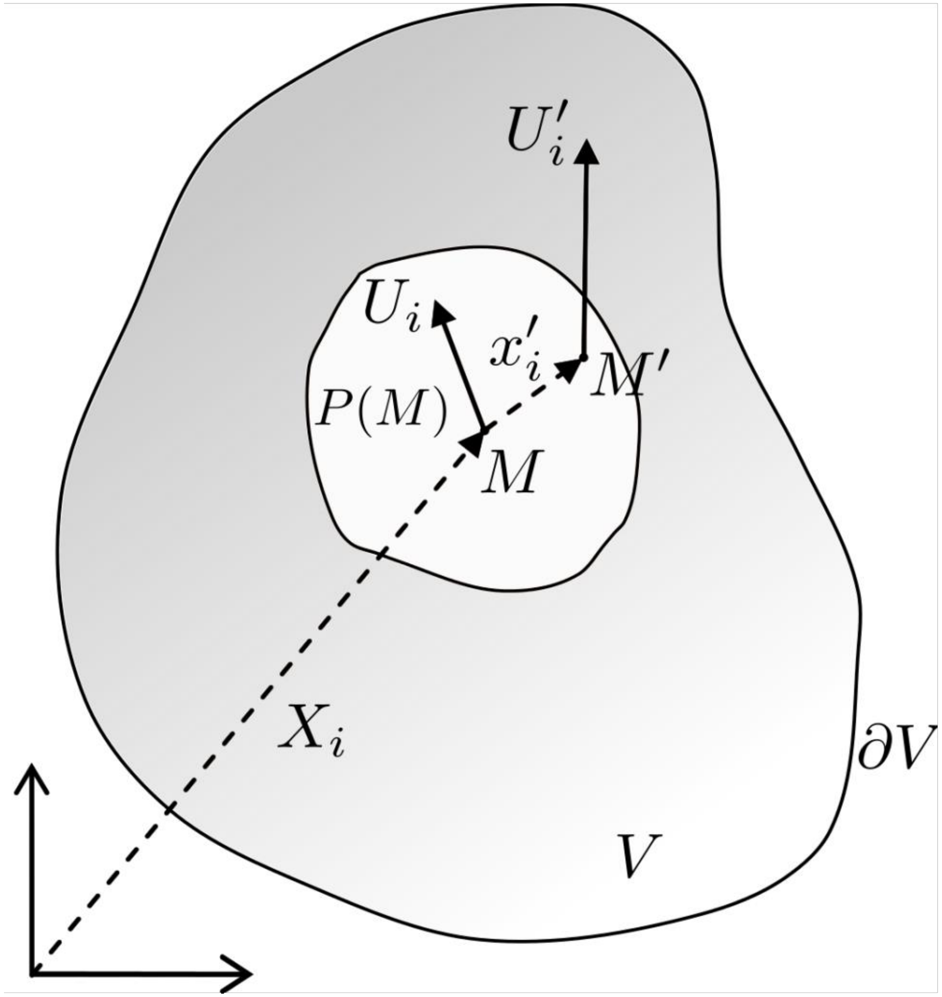

(Germain, 1973
Mindlin, 1964
Eringen, 1999,
…)

Ansatz:

$$U_i' = U_i + \chi_{ij} x_j' + \chi_{ijk} x_j' x_k' + \chi_{ijk\ell} x_j' x_k' x_\ell' + \ldots$$

Micromorphic continua

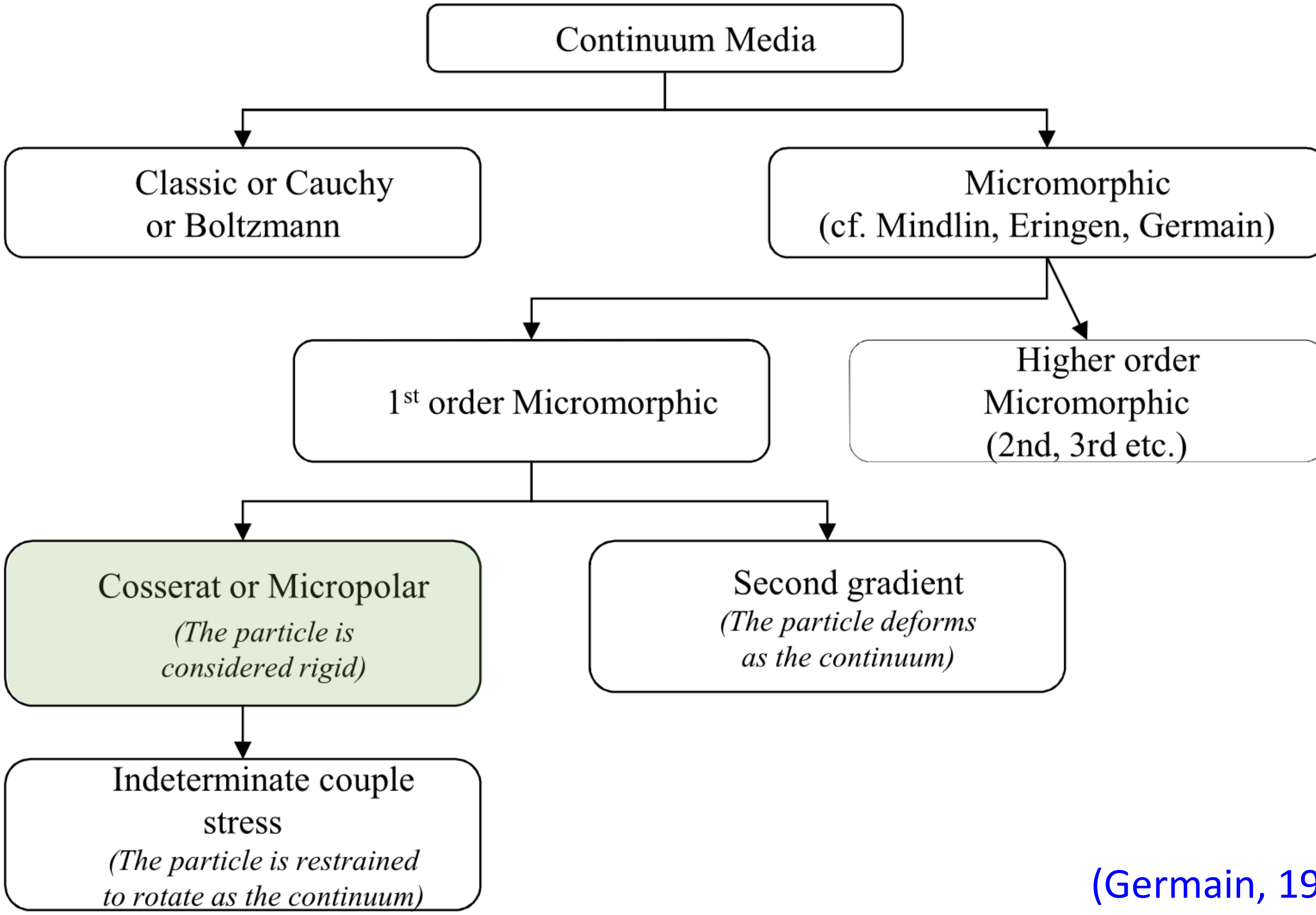

(Germain, 1973)

Linear and angular momentum balance for Cosserat

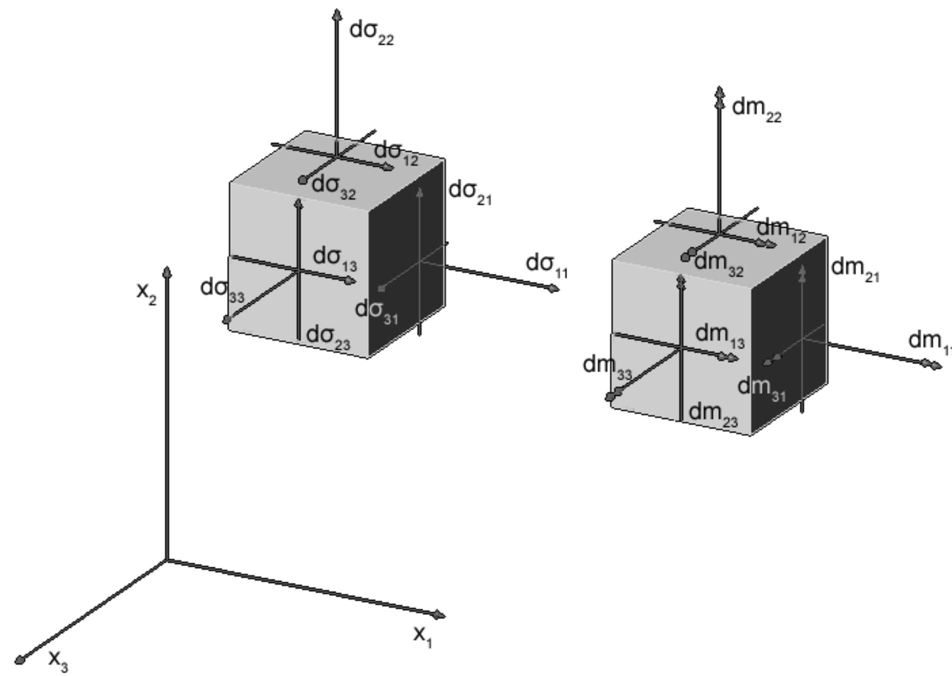

$$\sigma_{ij,j} = \rho \ddot{u}_i$$

$$m_{ij,j} + \varepsilon_{ijk}\sigma_{kj} = I_{ij}\ddot{\omega}_j^c$$

ε_{ijk} is the Levi-Civita symbol

σ_{ij} is the stress tensor (non-symmetric)

m_{ij} is the couple stress tensor

ρ is the density

I is the microinertia tensor

Why not the classical continuum ?

- Cosserat leads to a **finite shear band thickness**, as opposed to Cauchy continuum for which the shear band thickness is zero (unphysical).
- good representation of **softening** and **energy dissipation**, which controls temperature rise and other multiphysical couplings

Cauchy

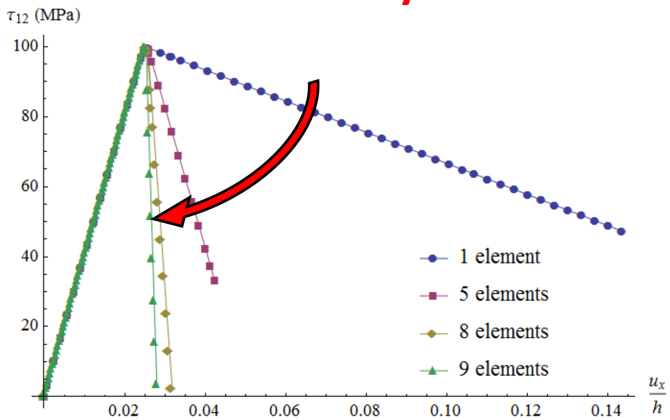

Cosserat

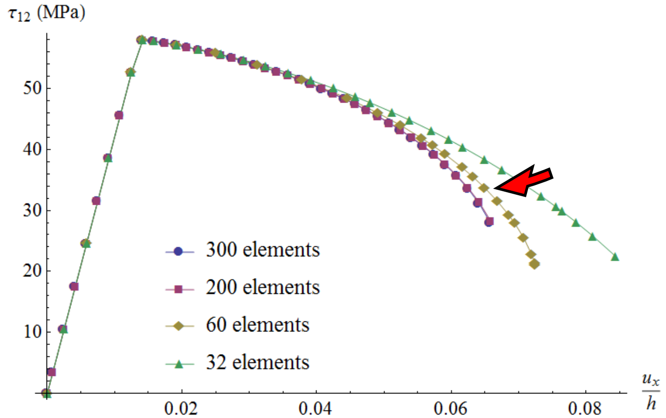

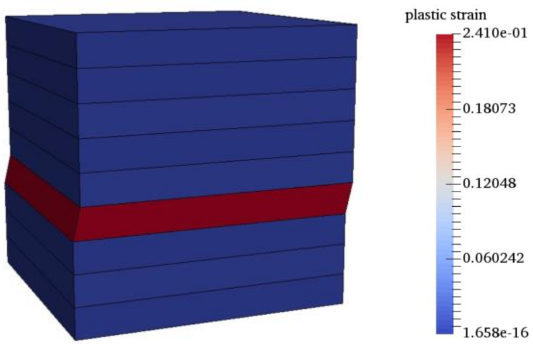

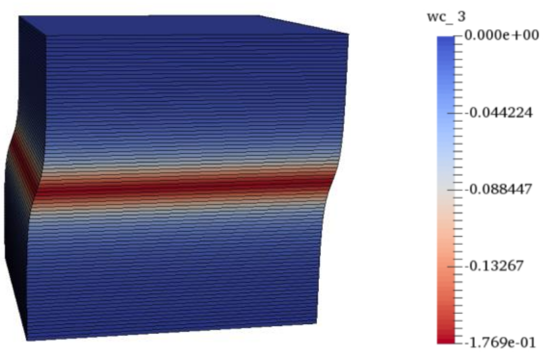

Physically based link of the localization thickness with the microstructure and its evolution (grain size and cataclasis)

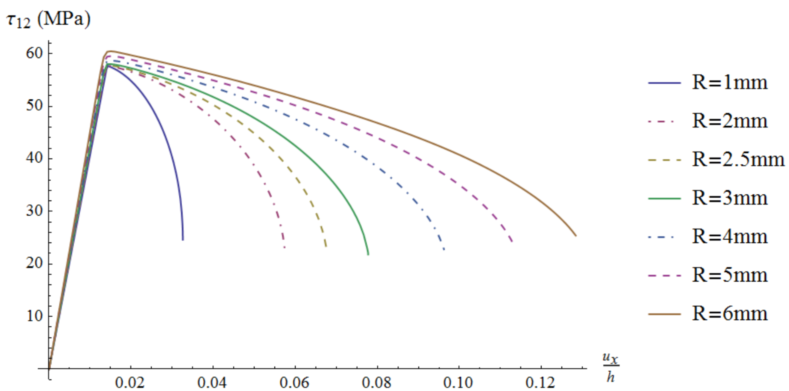

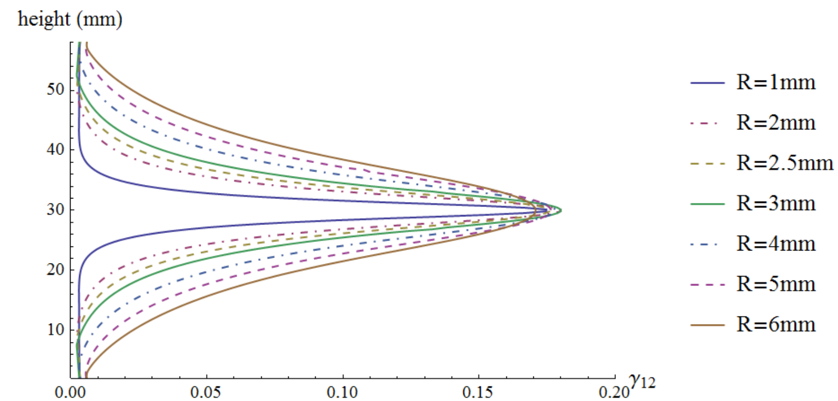

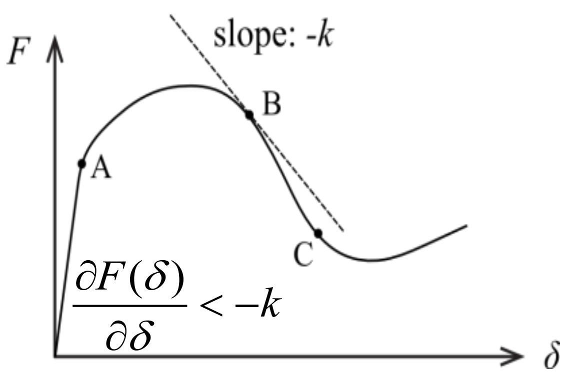

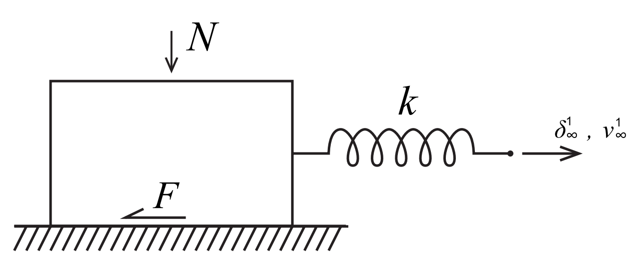

Mathematical modeling of fault zones

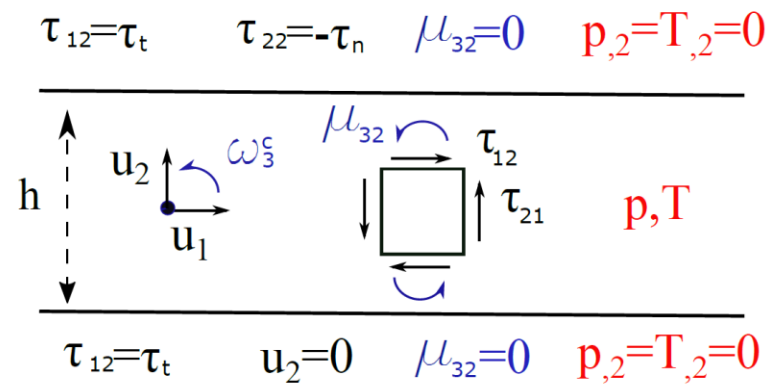

A fault zone is modelled as an infinite layer under shear.

Momentum balance equations:

$$\tau_{ij,j} - \rho \frac{\partial^2 U_i}{\partial t^2} = 0$$

$$\mu_{ij,j} - e_{ijk}\tau_{jk} - \rho I \frac{\partial^2 \omega_i^c}{\partial t^2} = 0$$

Elasto-plastic constitutive equation:

$$\dot{\tau}'_{ij} = C^{ep}_{ijkl}\ \dot{\gamma}_{kl} + D^{ep}_{ijkl}\ \dot{\kappa}_{kl} + E^{ep}_{ijkl}\ \dot{T}\ \delta_{kl}$$

$$\dot{\mu}_{ij} = M^{ep}_{ijkl}\ \dot{\kappa}_{kl} + L^{ep}_{ijkl}\ \dot{\gamma}_{kl} + N^{ep}_{ijkl}\ \dot{T}\ \delta_{kl}$$

Terzaghi effective stress: $\tau'_{ij} = \tau_{ij} + p\ \delta_{ij}$

Energy balance equation:

$$\frac{\partial T}{\partial t} - c_{th} T_{,ii} = \frac{1}{\rho C} \underbrace{(\sigma_{ij}\dot{\varepsilon}^p_{ij} + \mu_{ij}\dot{\kappa}^p_{ij})}_{\text{Plastic work}}$$

Mass balance equation:

$$\frac{\partial p}{\partial t} = c_{hy}\ p_{,ii} + \underbrace{\frac{\lambda^*}{\beta^*}\frac{\partial T}{\partial t}}_{\text{Thermal pressurisation}} - \underbrace{\frac{1}{\beta^*}\frac{\partial \varepsilon_v}{\partial t}}_{\text{Porosity variation}}$$

Cosserat continuum (J2) plasticity

- Drucker-Prager yield surface (Mülhaus & Vardoulakis, 1987) with hardening

$$F = \tau + \mu\sigma' - c$$

$$Q = \tau + \beta\sigma'$$

$$H_s = -\frac{d\mu}{d\gamma^p}\sigma'$$

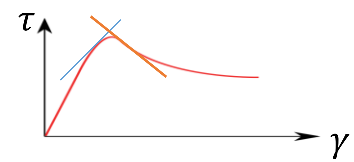

- Generalized stress and strain invariants

$$\tau = \sqrt{h_1\, s_{ij}\, s_{ij} + h_2\, s_{ij}\, s_{ji} + \frac{1}{R^2}(h_3\, \mu_{ij}\, \mu_{ij} + h_4\, \mu_{ij}\, \mu_{ji})}$$

$$\gamma^p = \sqrt{g_1\, e^p_{ij}\, e^p_{ij} + g_2\, e^p_{ij}\, e^p_{ji} + R^2(g_3\, \kappa^p_{ij}\, \kappa^p_{ij} + g_4\, \kappa^p_{ij}\, \kappa^p_{ji})}$$

s_{ij} and e^p_{ij} are, respectively, the deviatoric part of the stress and the plastic strain.
R is the internal length.
h_i and g_i are coefficients determined by micro-mechanical considerations.

Bifurcation and linear stability analysis

Linearization of the non-linear system around the homogeneous steady state: $\bar{T}$, $\overline{\gamma_{ij}}$, $\bar{p}$.

$$T(z,t) = \bar{T} + T^*(z,t)$$
$$\gamma_{ij}(z,t) = \overline{\gamma_{ij}} + \gamma_{ij}^*(z,t)$$
$$\mathrm{p}(z,t) = \bar{p} + p^*(z,t)$$

General solution of the linearized system:

$$T^*(z,t) = \Theta \exp(s.t) \exp(2\pi i \frac{z}{\lambda})$$

$$\gamma_{ij}^*(z,t) = \mathrm{E}_{ij} \exp(s.t) \exp(2\pi i \frac{z}{\lambda})$$

$$p^*(z,t) = P \exp(s.t) \exp(2\pi i \frac{z}{\lambda})$$

Onset of strain localization: **Re(s)>0**

Unstable $s > 0$

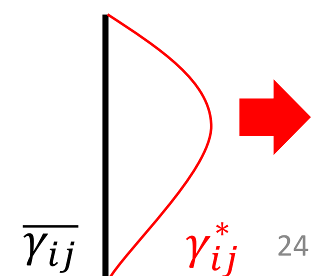

Bifurcation parameter and hardening

⇨ Bifurcation for a hardening modulus H_{cr}

Stable case

$H_s = 2{,}81\ MPa$

s

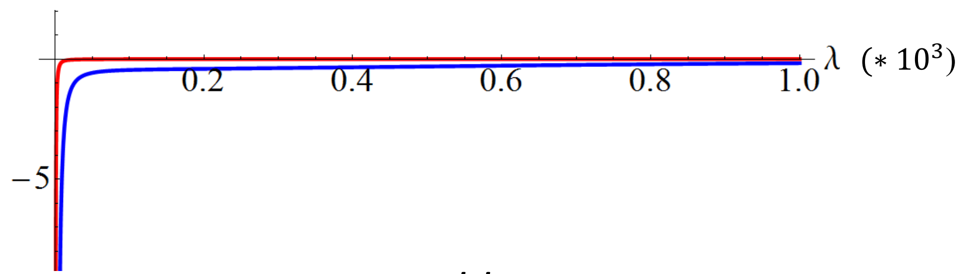

Unstable case

$H_s = 2{,}8\ MPa > \mathbf{0}$

s

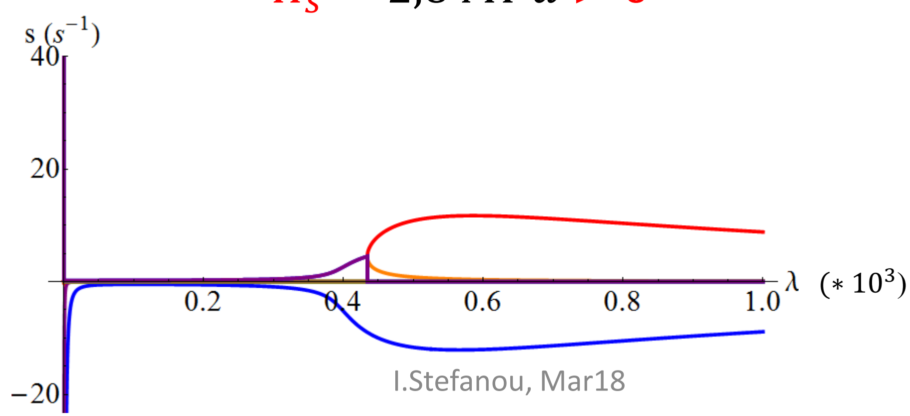

Onset of strain localization and couplings

- The parameter that most influences the bifurcation is the dilatancy β.

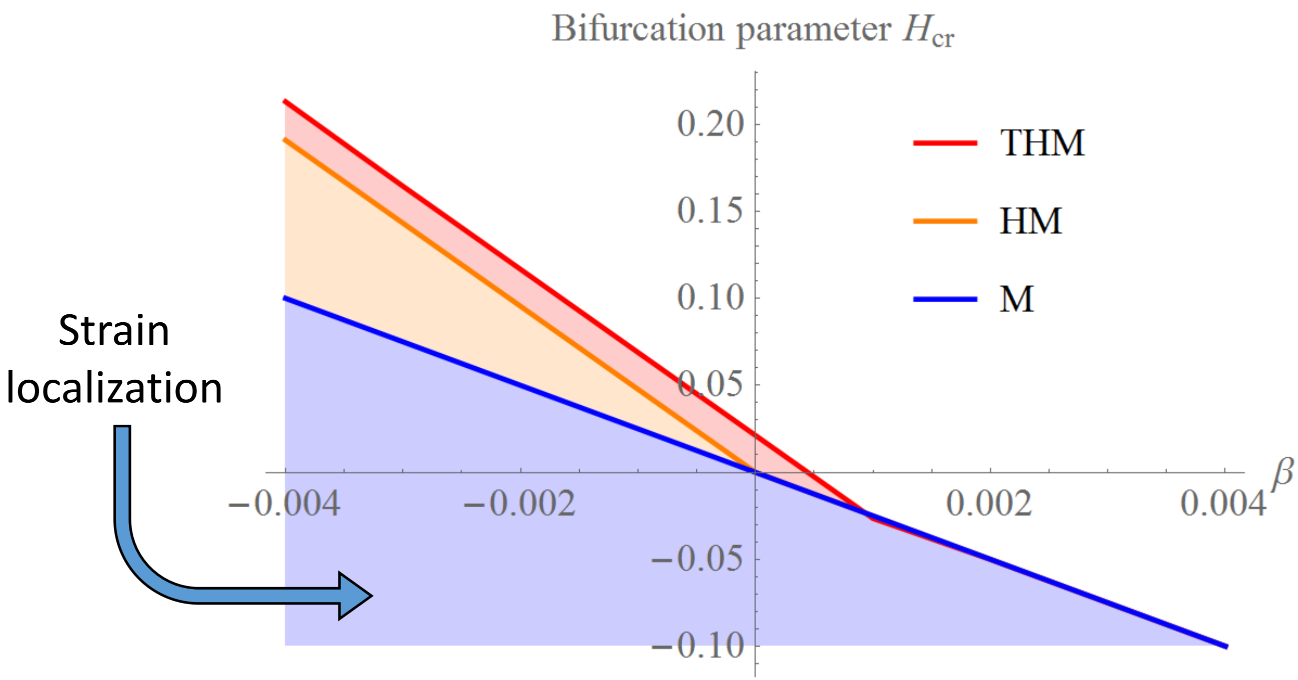

Rattez et al. 2018, JMPS

- HM couplings destabilize the system for contractant materials (β<0).
- THM couplings make the system unstable for dilatant materials in the hardening regime.

Wavelength selection and thickness of the band

Evolution of the maximum *s(λ)* with the hardening modulus

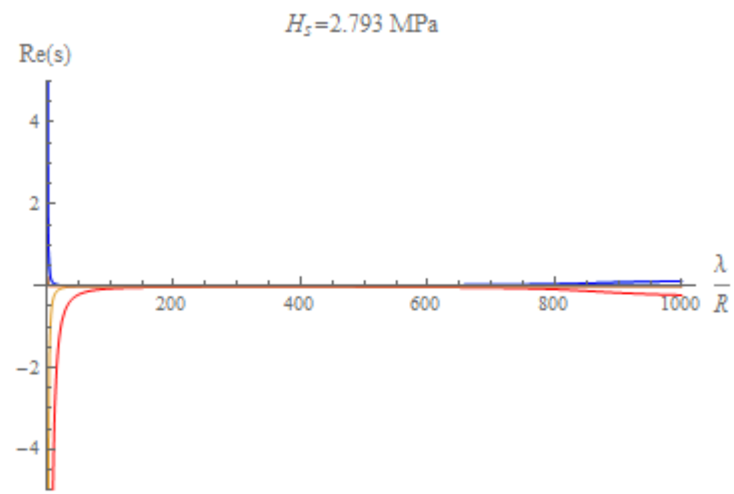

Evolution of the shear band thickness in function of the hardening modulus

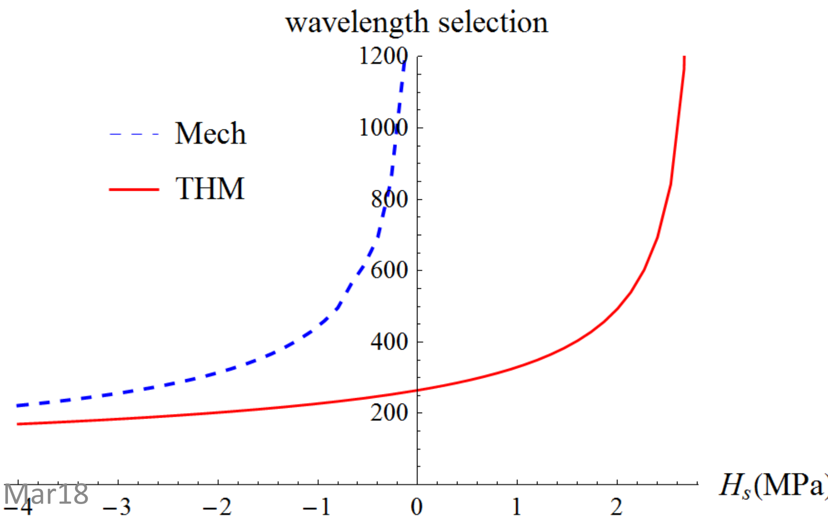

Shear band thickness evolution with shear deformation

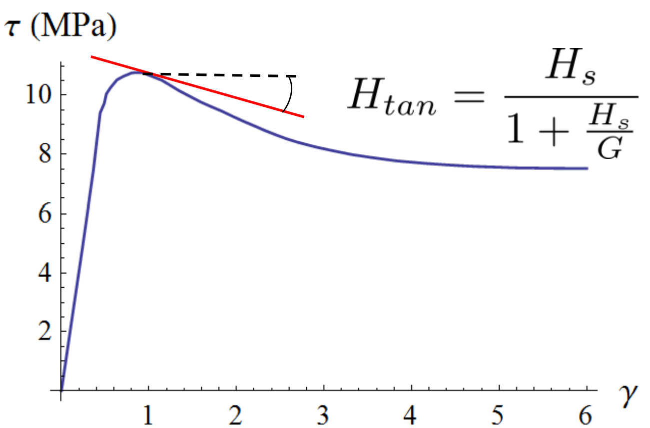

(Ikari et al.,2008)

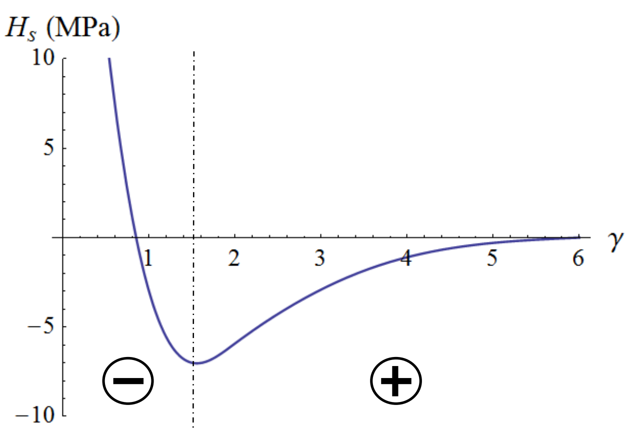

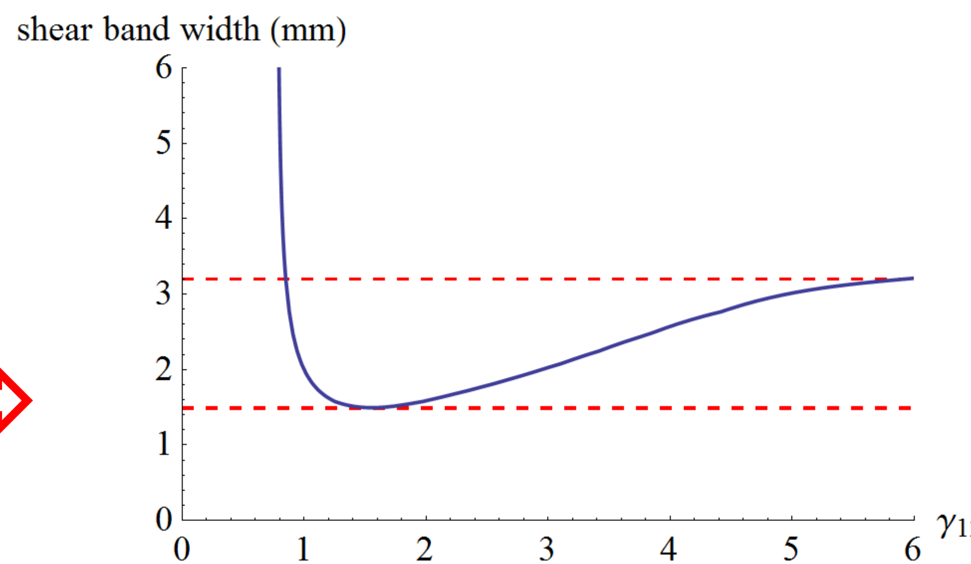

Effect of grain cataclasis during shearing

Supposing an exponential evolution of D_{50} with the total shear strain γ.

$$D(\gamma) = (D_0 - D_{fin})e^{-\frac{\gamma}{\gamma_c}} + D_{fin}$$

Progressive decrease of the shear band thickness.

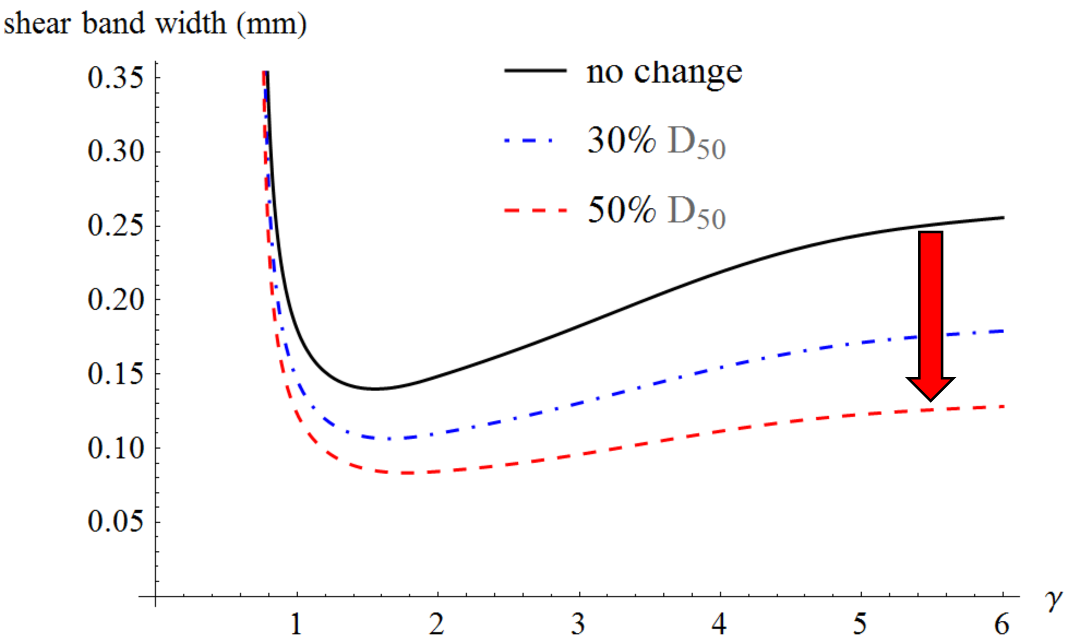

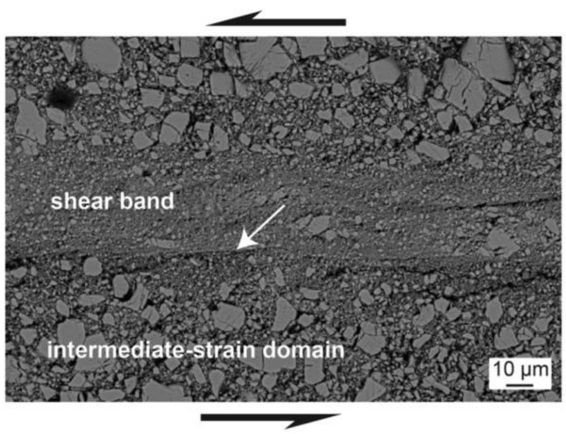

Shear band in Dolomite, tested with a rotary shear apparatus (Smith et al., 2015)

FEM analysis of Cosserat THM model

The full system of equations is integrated numerically using a displacement-rotation finite element formulation
(Rattez et al. 2018a&b, JMPS)

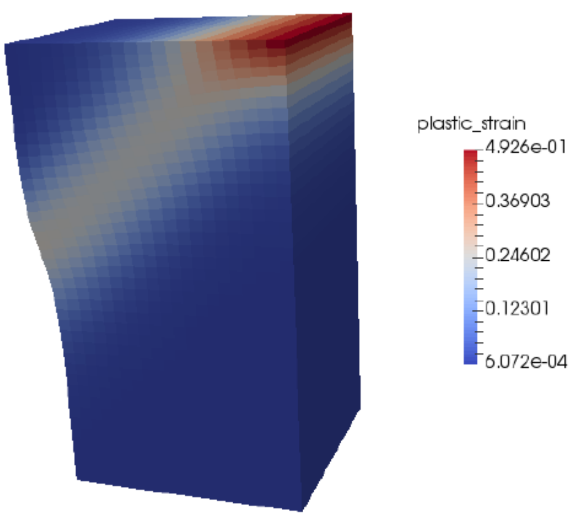

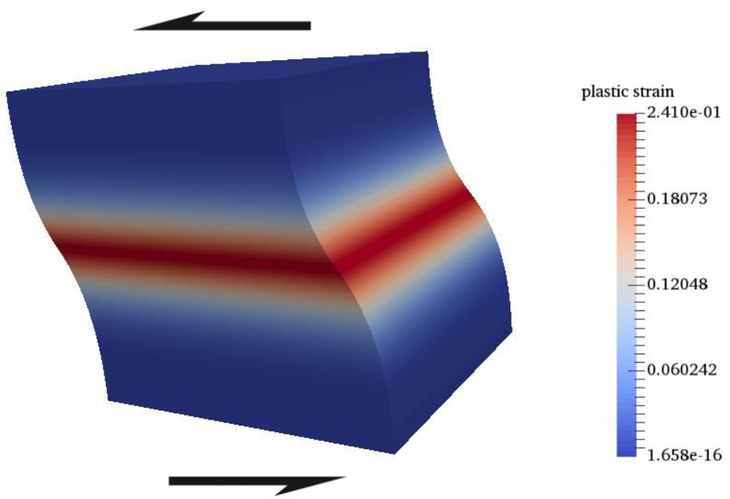

FEM formulation

- Weak form of the momentum balance equations:

$$-\int_{\Omega} \tau_{ij}\psi_{i,j} d\Omega + \int_{\partial\Omega_\Sigma} \tau_{ij} n_j \psi_i dS = 0$$

$$-\int_{\Omega} \mu_{ij}\psi_{i,j} d\Omega + \int_{\partial\Omega_\Sigma} \mu_{ij} n_j \psi_i dS - \int_{\Omega} \varepsilon_{ijk}\tau_{jk}\psi_i d\Omega = 0$$

- Weak form of energy and mass balance equations:

$$\int_{\Omega} \dot{p}\psi d\Omega + c_{hy}\left(\int_{\Omega} p_{,i}\psi_{,i} d\Omega - \int_{\partial\Omega} p_{,i} n_i \psi dS\right) - \Lambda \int_{\Omega} \dot{T}\psi d\Omega + \frac{1}{\beta^*}\int_{\Omega} \dot{\varepsilon_v}\psi d\Omega = 0$$

$$\int_{\Omega} \dot{T}\psi d\Omega + c_{th}\left(\int_{\Omega} T_{,i}\psi_{,i} d\Omega - \int_{\partial\Omega} T_{,i} n_i \psi dS\right) - \frac{1}{\rho C}\int_{\Omega} (\tau_{ij}\dot{\gamma}^p_{ij} + \mu_{ij}\dot{\kappa}^p_{ij})\psi_{,i} d\Omega = 0$$

- ψ and ψ_i are linear or quadratic Lagrange test functions.

- The incremental plastic constitutive law is integrated using a return map algorithm (Godio et al., 2016).

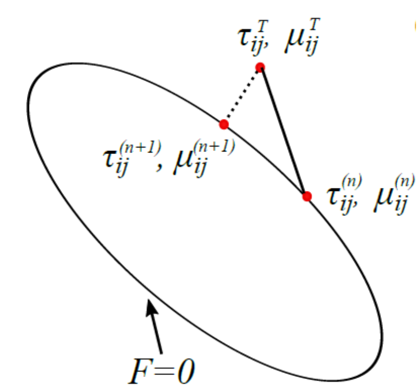

Numerical results

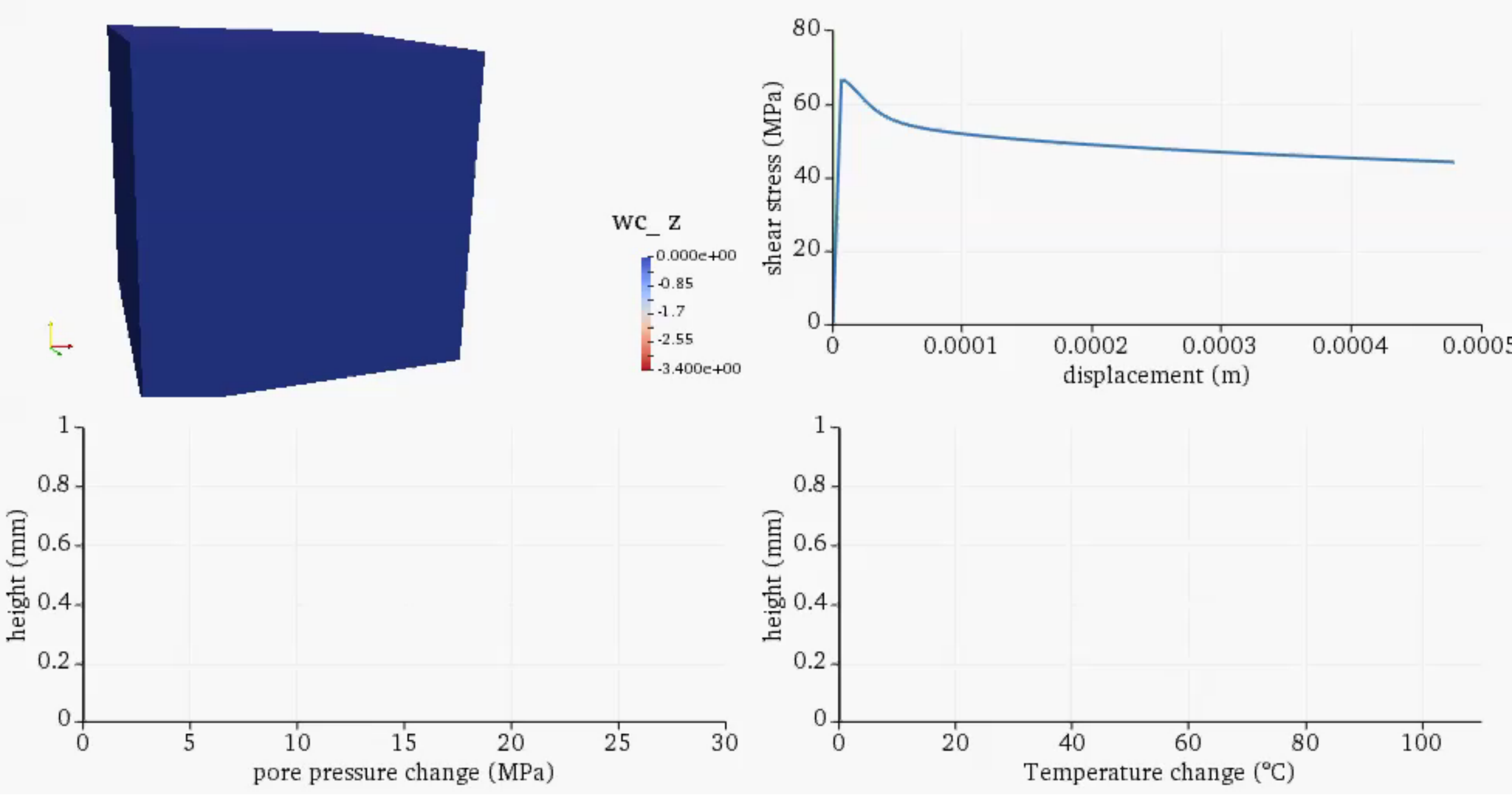

Effect of the grain size

The grain size affects the shear band thickness

and the stress-strain diagram.

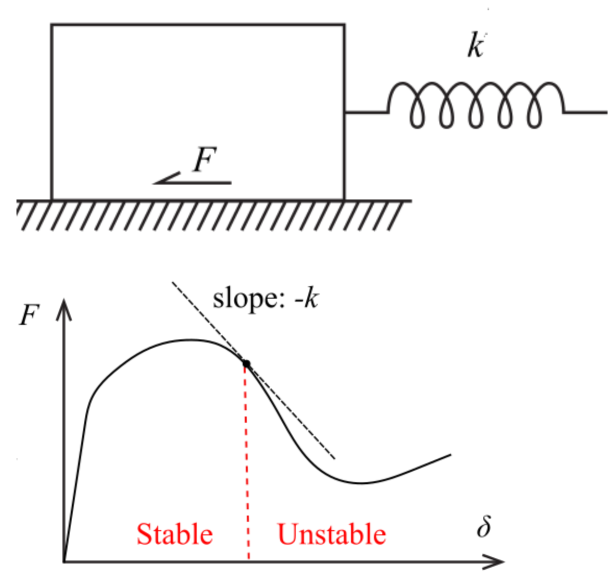

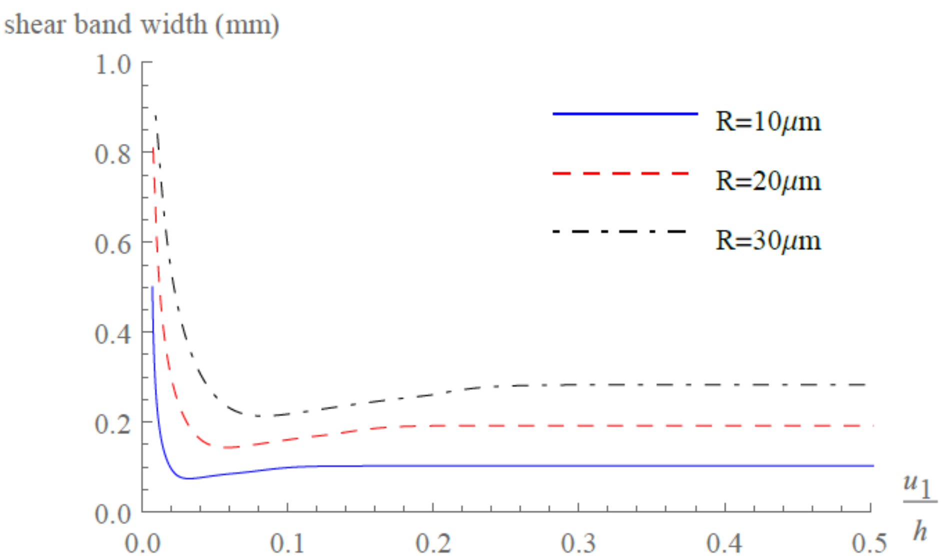

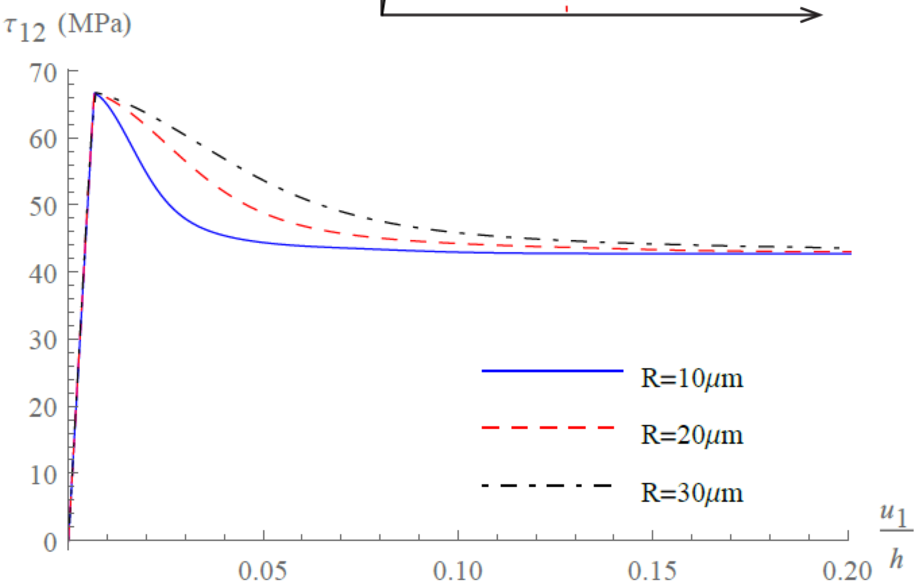

Apparent rate-dependency

...despite the use of a rate-independent constititutive law (perfect plasticity here).

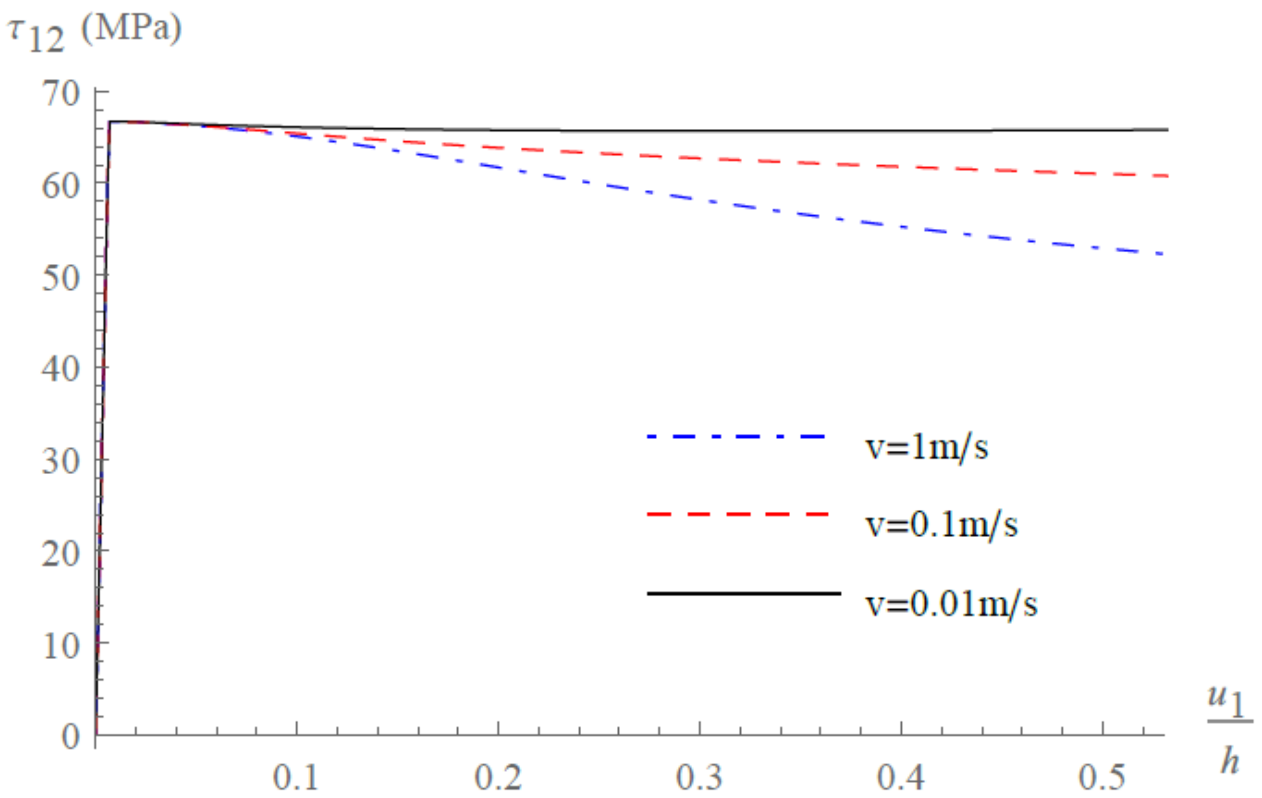

Slow shearing

Fast shearing

Rate-dependency of strain localization thickness

Diffusion processes change the localization thickness

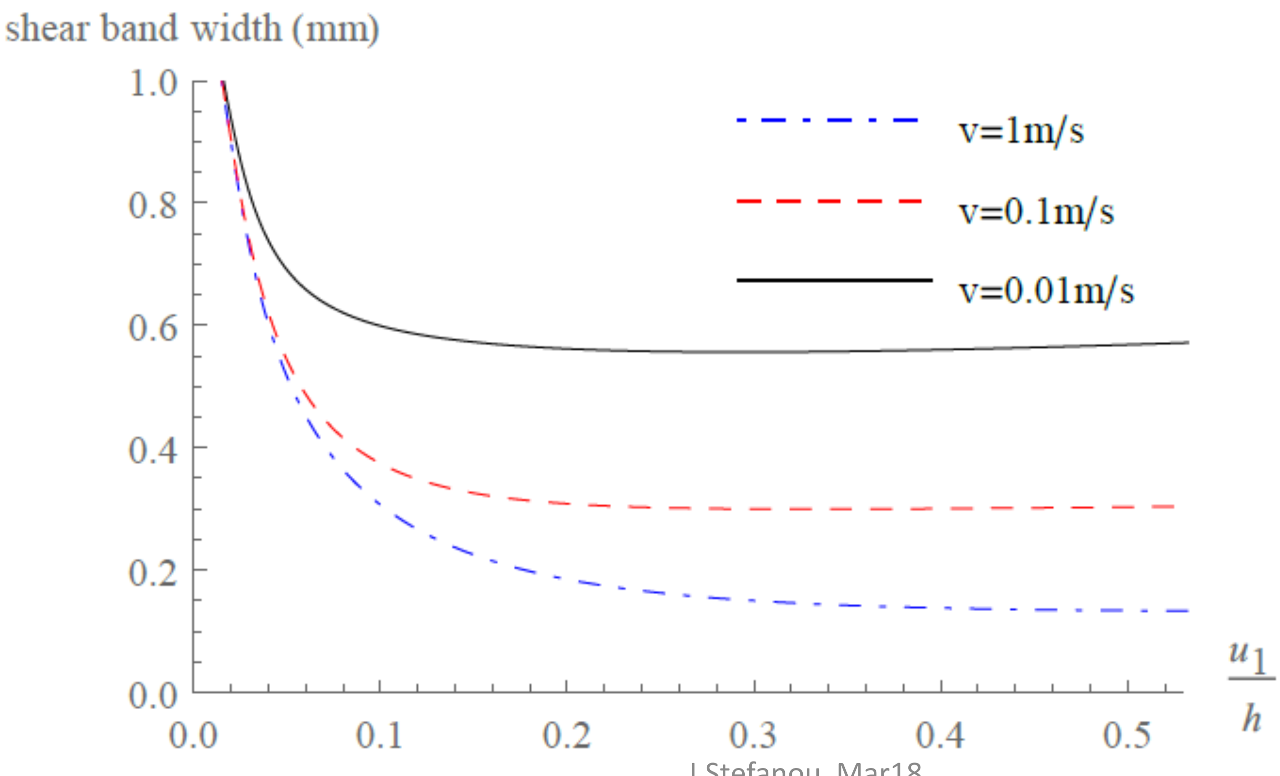

Slow shearing

Fast shearing

Fast rate (1 m/s)

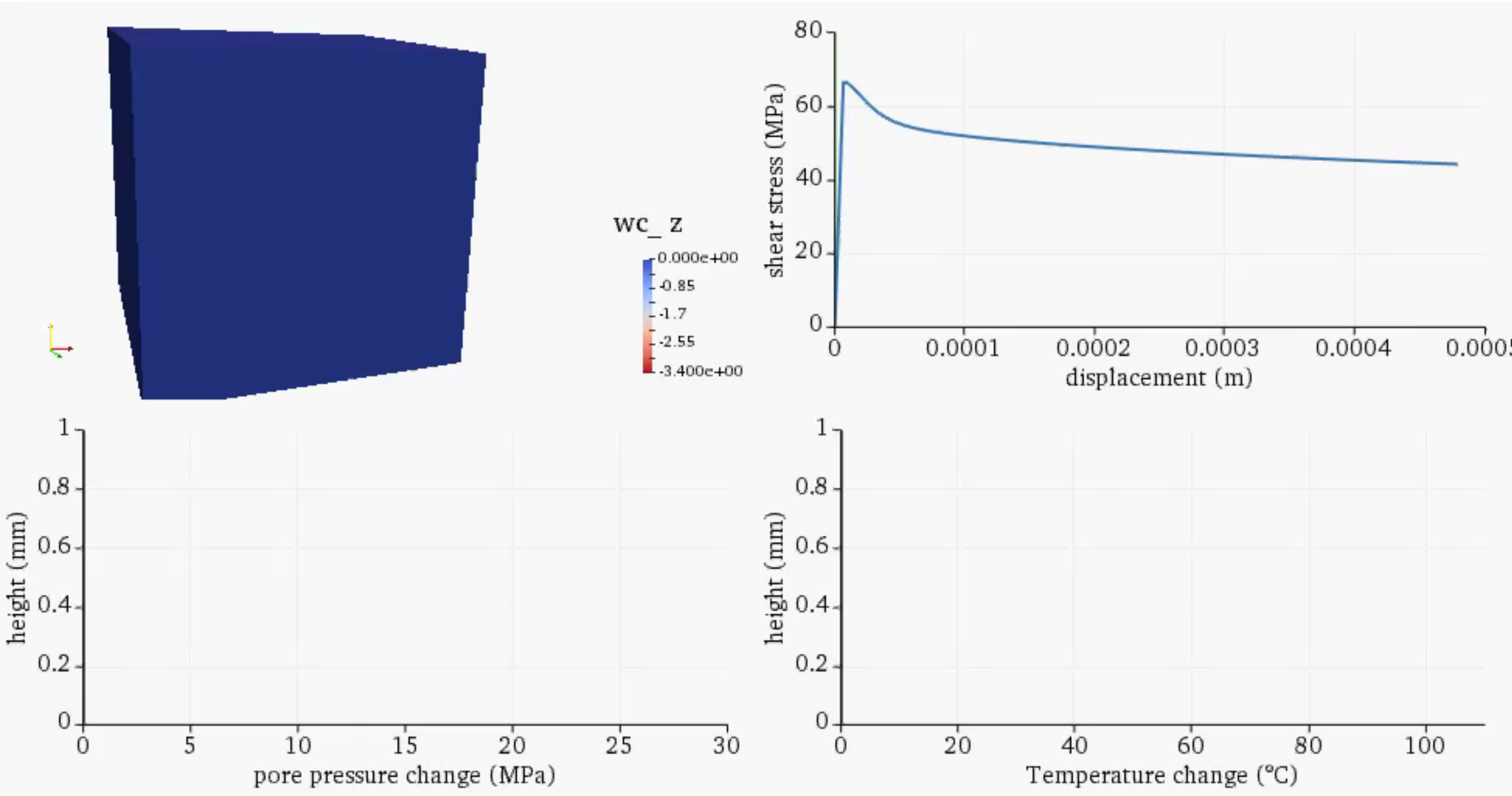

Slow rate (0.01 m/s)

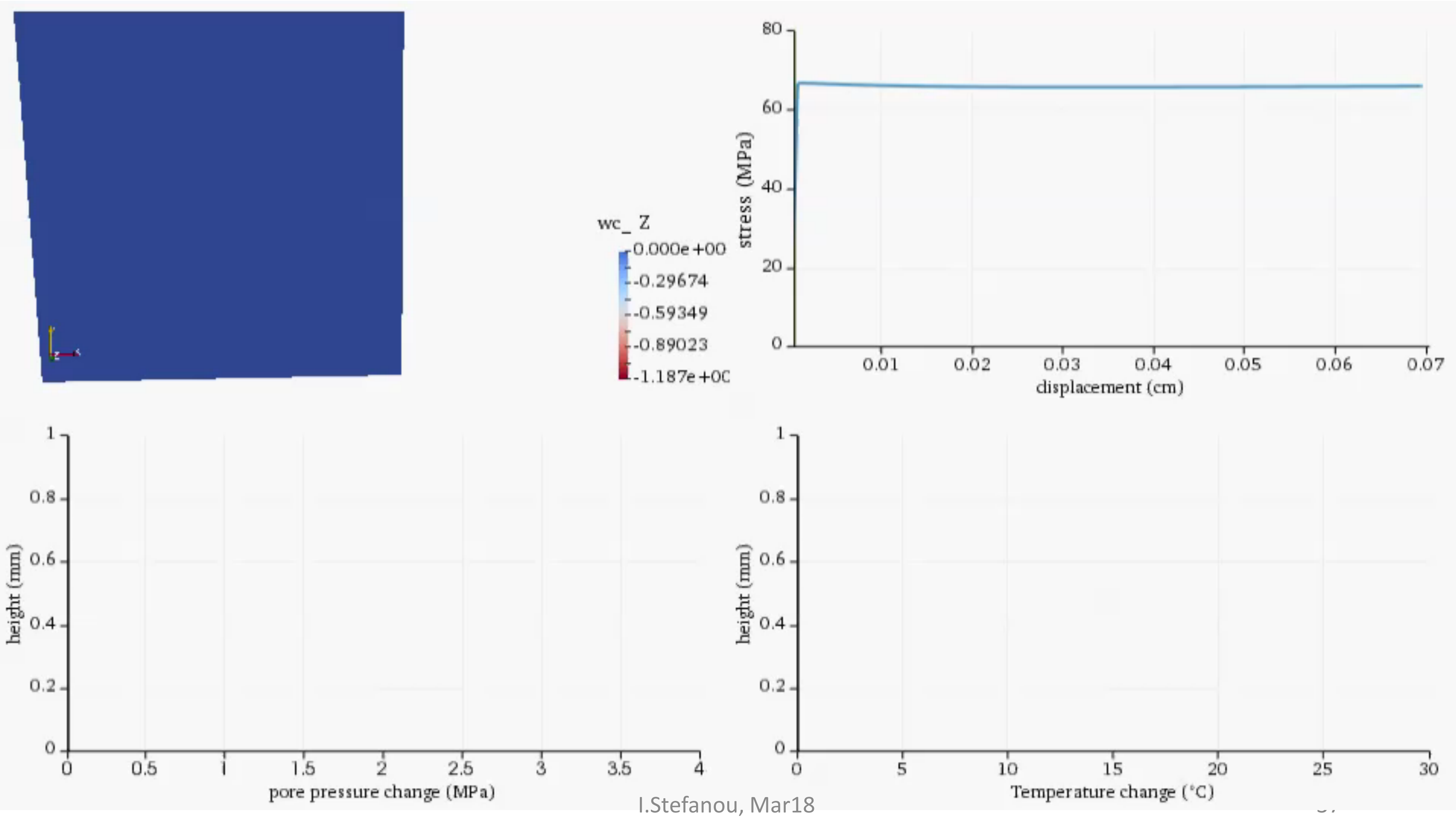

Comparison with field observations

In situ observations of the Punchbowl fault (San Andreas system, southern California) show that the Principal Slip Zone (PSZ) is 100-300μm thick.

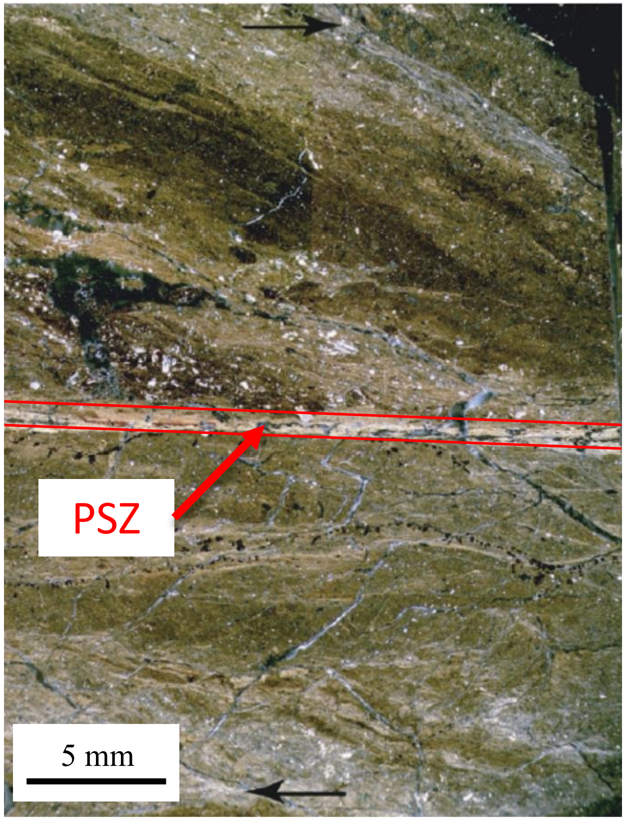

Chester et al. (2005), Rice (2006)

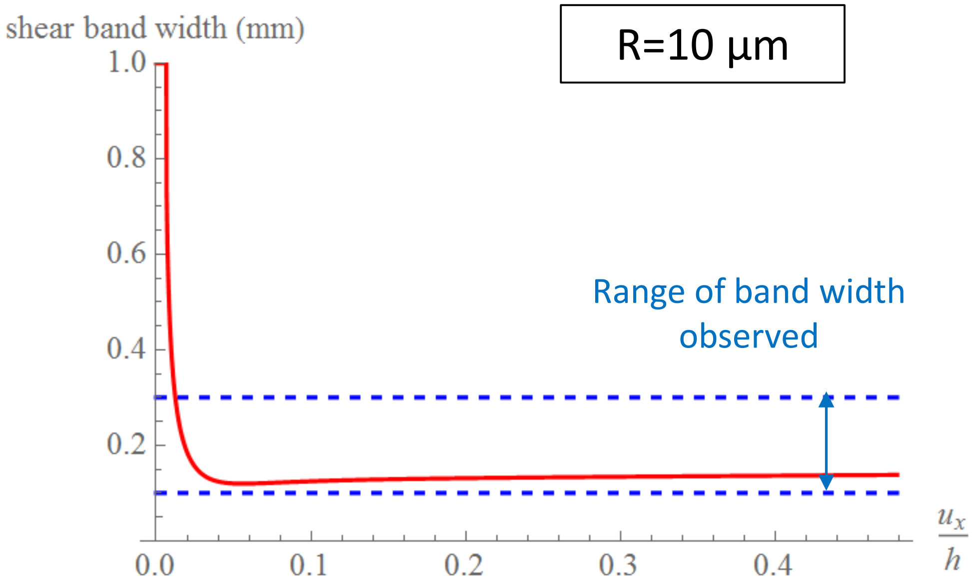

⇨ Shear band thickness prediction consistent with field observations of the Punchbowl fault.

Can modeling be predictive?

Laboratory tests ?

Different thermo-hydro-chemo-mechanical conditions down there (several km's)…

In-situ measurements?

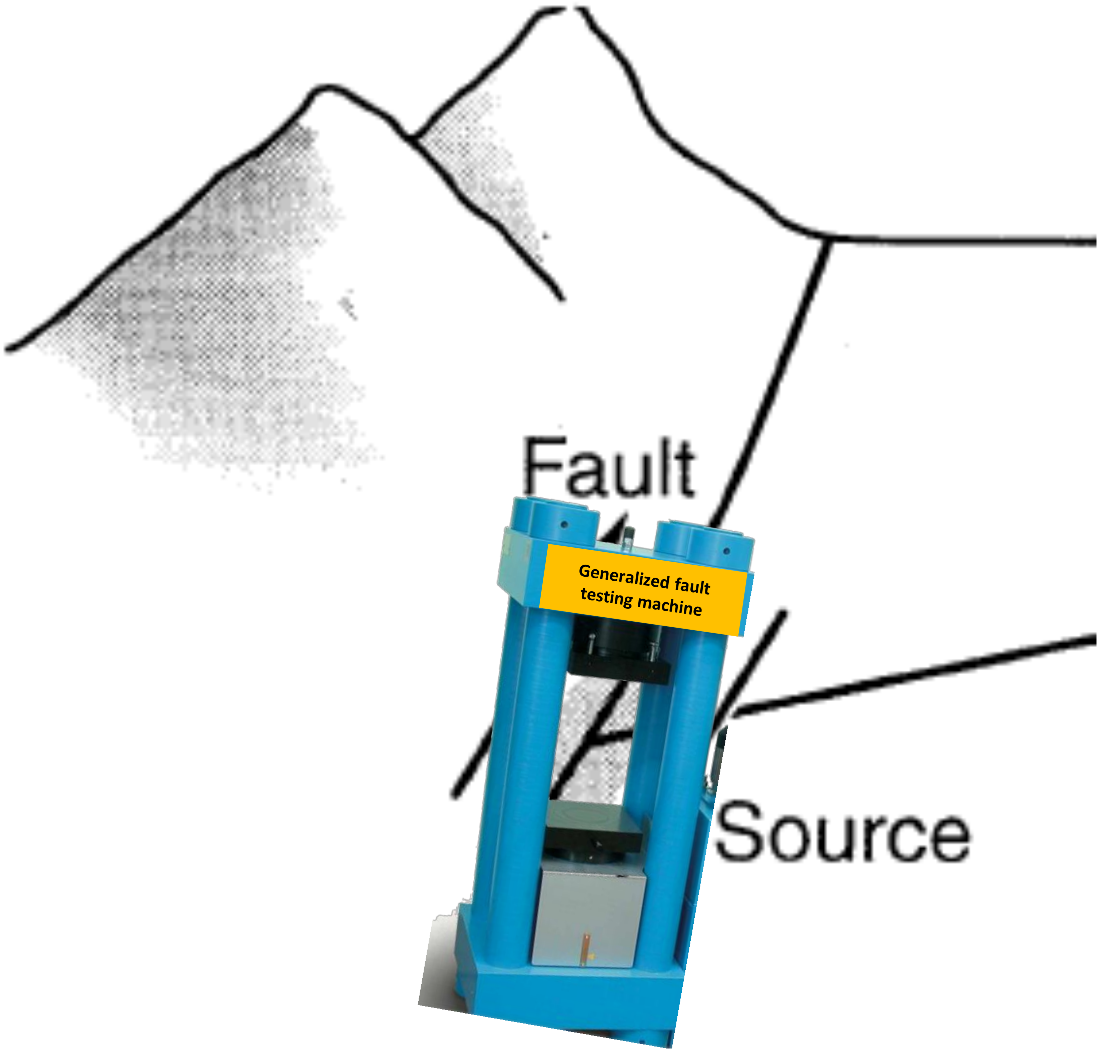

If we could, could we avoid earthquakes?

ERC Starting Grant:

Controlling earthQuakes

(CoQuake)

CoQuake

Engineer for the **Parthenon** at the end of PhD and early Post-Doc;

earthquake effects and **seismic design**

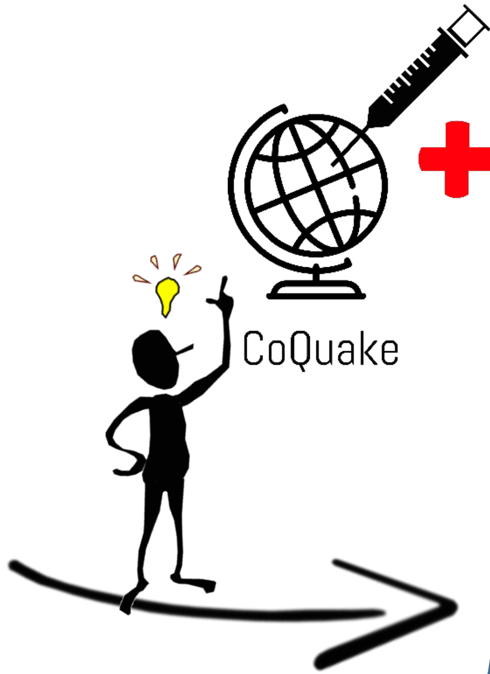

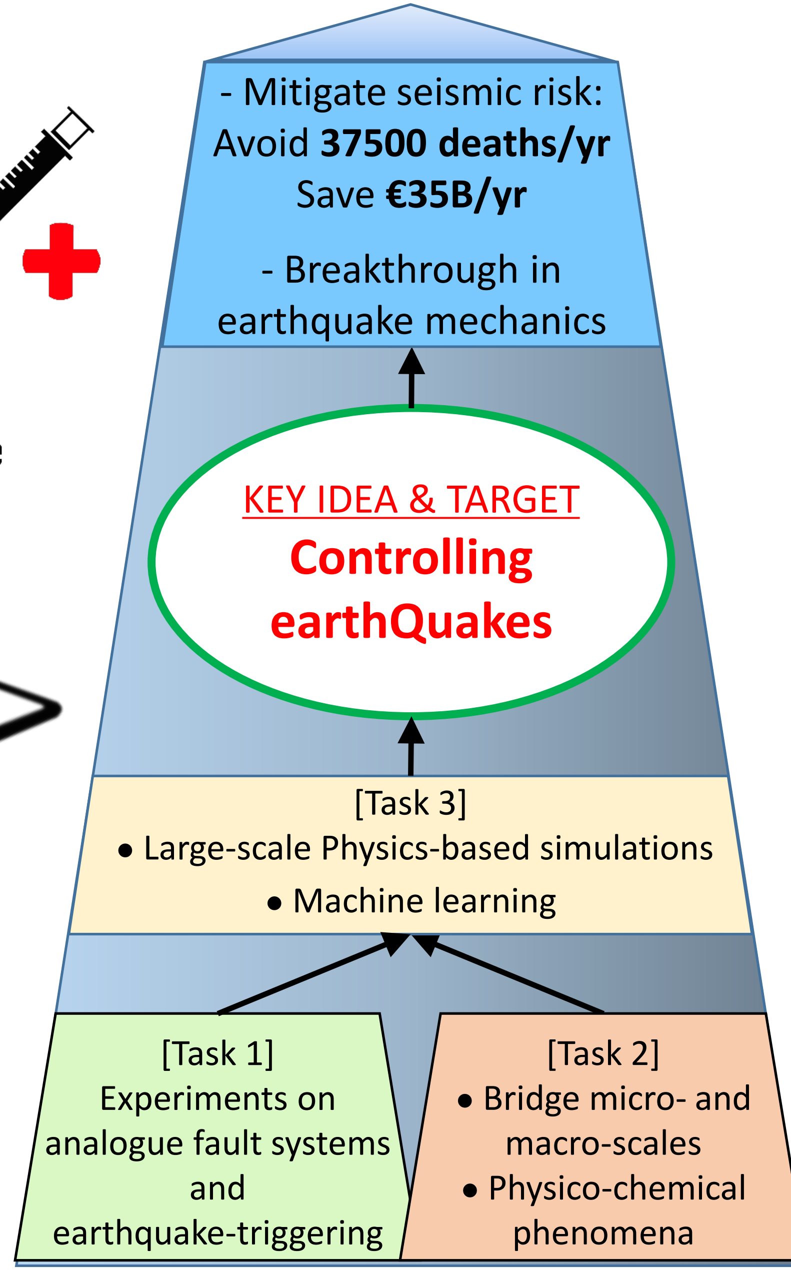

Earthquake control

Humans cause earthquakes

(review: Rubinstein & Mahani SRL2015, McGarr JGR2014, Ellsworth, Science2013)

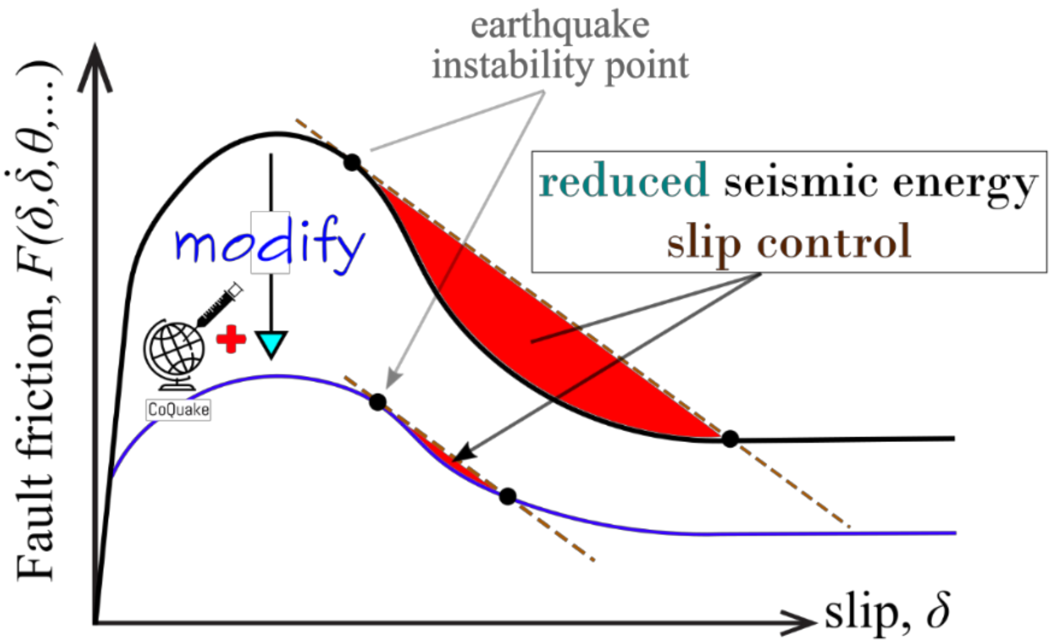

Trigger instability on a

lower energy level

Going back to Nepal

Fault patch characteristics
Total slip area: ~3500km^2
Central slip area: dipping: ~10km, ~horizontal: ~100km

CoQuake:
- ✓ Inland (lower cost)
- ✓ Accessible depth by drilling

Order of magnitude of drilling cost @ that depth and span (current prices & state of technology): 100 million

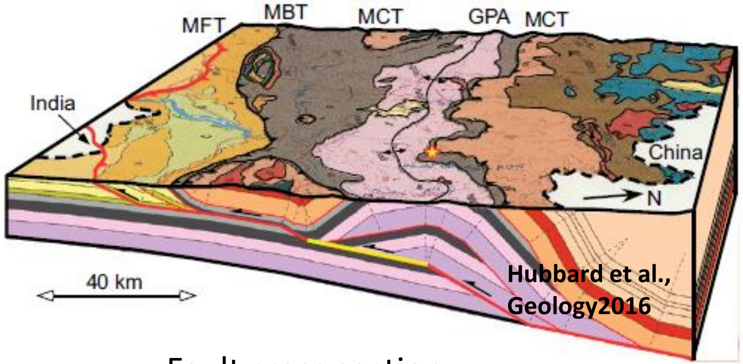

Fault cross section

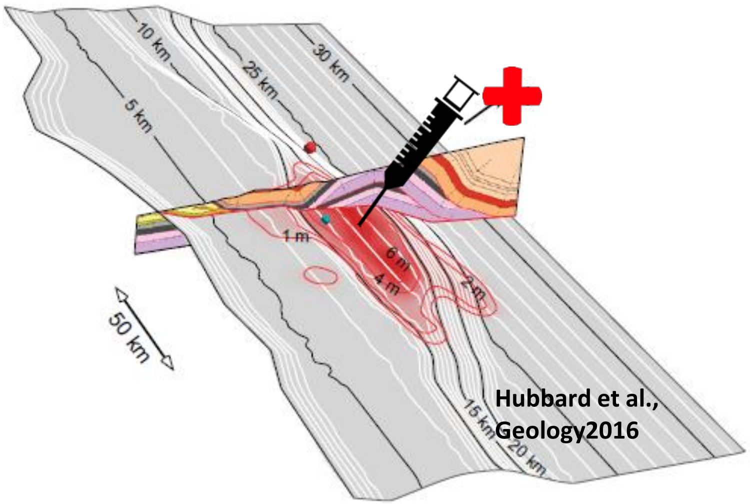

Perspective view of fault

Thank you for your attention

ioannis.stefanou@enpc.fr

Related references:

Rattez, H., Stefanou, I., Sulem J. et al. (2018), Validation of the THM Cosserat model, submitted to RMRE

Rattez, H., Stefanou, I., & Sulem, J. (2018). The importance of Thermo-Hydro-Mechanical couplings and microstructure to strain localization in 3D continua with application to seismic faults. Part I: Theory and linear stability analysis. JMPS

Rattez, H., Stefanou, I., Sulem, J., Veveakis, M., & Poulet, T. (2018). The importance of Thermo-Hydro-Mechanical couplings and microstructure to strain localization in 3D continua with application to seismic faults. Part II: Numerical implementation and post-bifurcation analysis. JMPS

Stefanou, I., Sulem, J., & Rattez, H. (2017). Cosserat approach to localization in geomaterials. In Handbook of Nonlocal Continuum Mechanics for Materials and Structures. Springer.

Godio, M., Stefanou, I., Sab, K., Sulem, J., & Sakji, S. (2016). A limit analysis approach based on Cosserat continuum for the evaluation of the in-plane strength of discrete media: application to masonry. European Journal of Mechanics - A/Solids, 66, 168–192.

Sulem, J., & Stefanou, I. (2016). Thermal and chemical effects in shear and compaction bands. Geomechanics for Energy and the Environment, 6, 4–21.

Stefanou, I., & Sulem, J. (2016). Existence of a threshold for brittle grains crushing strength: two-versus three-parameter Weibull distribution fitting. Granular Matter, 18(2), 14.

Godio, M., Stefanou, I., Sab, K., & Sulem, J. (2016). Multisurface plasticity for Cosserat materials: Plate element implementation and validation. International Journal for Numerical Methods in Engineering, 108(5), 456–484.

Godio, M., Stefanou, I., Sab, K., & Sulem, J. (2015). Dynamic finite element formulation for Cosserat elastic plates. International Journal for Numerical Methods in Engineering, 101(13), 992–1018.

Stefanou, I., & Sulem, J. (2014). Chemically induced compaction bands: Triggering conditions and band thickness. Journal of Geophysical Research: Solid Earth, 119(2), 880–899.

Veveakis, E., Stefanou, I., & Sulem, J. (2013). Failure in shear bands for granular materials: thermo-hydro-chemo-mechanical effects. Géotechnique Letters, 3(April-June), 31–36.

Veveakis, E., Sulem, J., & Stefanou, I. (2012). Modeling of fault gouges with Cosserat Continuum Mechanics: Influence of thermal pressurization and chemical decomposition as coseismic weakening mechanisms. Journal of Structural Geology, 38, 254–264.

Sulem, J., Stefanou, I., & Veveakis, E. (2011). Stability analysis of undrained adiabatic shearing of a rock layer with Cosserat microstructure. Granular Matter, 13(3), 261–268.

Stefanou, I., Sulem, J., & Vardoulakis, I. (2008). Three-dimensional Cosserat homogenization of masonry structures: elasticity. Acta Geotechnica, 3(1), 71–83.

Stefanou, I., Sulem, J., & Vardoulakis, I. (2010). Homogenization of interlocking masonry structures using a generalized differential expansion technique. International Journal of Solids and Structures, 47(11–12), 1522–1536.